Thermochimica Acta, 75 (1984) 361–399
Elsevier Science Publishers B.V., Amsterdam – Printed in The Netherlands

Review

EVOLVED GAS ANALYSIS BY MASS SPECTROMETRY: A REVIEW

MACK R. HOLDINESS

Louisiana State University Medical Center, Department of Pharmacology and Experimental Therapeutics, 1901 Perdido Street, New Orleans, LA 70112 (U.S.A.)

(Received 11 October 1983)

CONTENTS

A. INTRODUCTION

In the last thirty years the field of chemistry has seen much of the development of techniques of evolved gas analysis (EGA) by mass spectrometry (MS). This methodology (EGA-MS) has progressed from simple heating of samples deposited on an inert matrix and observing the decomposition products leaked into an ion source [1] to automated simultaneous monitoring of three thermal analytical techniques by MS [2]. The exact nature of the evolved gases is unknown when observed only by thermal analysis (TA); however, coupled with MS it provides a powerful means of sample identification and quantitation. When MS is used in conjunction with thermogravimetry (TG) or differential thermal analysis (DTA) it may provide information concerning the reacting system itself.

Excellent reviews of this subject were written in 1967 by Langer and Gohlke [3] and in 1970 by Friedman [4]. The material contained in this report represents advances that have been published since that time. In this review the instrumentation for EGA-MS will be discussed along with selected applications in inorganic, organic, polymer, geological and biological chemistry.

0040-6031/84/$03.00

B. INSTRUMENTATION AND SELECTED APPLICATIONS

(i) Pyrolysis techniques

The oldest and most widely used method is the heating of a sample until gaseous breakdown products are evolved, which may be monitored by MS. These pyrolyzed gases can be generated in the ion source by direct probe insertion or outside the MS and admitted by appropriate mechanical means. Techniques for sample production include coating materials on filaments which are heated in varying steps [5], Curie-point pyrolysis [6], direct probe insertion [7,8], remote pyrolysis by a tube furnace [9], Knudsen cells [10], expansion bulb leakage [11] and flash vacuum thermolysis [12]. Specialized methods of laser pyrolysis [13] and laser microprobe mass analyzer (LAMMA) [14,15] are utilized to allow fingerprinting of samples as small as 10^{-12} g. For reviews on the application of analytical pyrolysis the reader is referred to Irwin [16,17], Berezkin [18] and Irwin and Slack [19].

By direct insertion probe (DIP) pyrolysis MS a sample is heated at a controlled rate (linear programmed or ballistic) and the total ion current of the MS monitored. Mass spectra may be recorded at appropriate points as the decomposition products are evolved, or selected ions may be monitored to follow the relationship of a characteristic component to the total ion output. The merit of DIP depends to a large extent upon the samples under investigation. At best, the decomposition occurs in a stepwise manner in which each intermediate decomposes in turn, therefore providing information about the reacting system itself. However, at the opposite extreme the sample is volatilized in the source, yielding limited data about the thermal decomposition process. For practical considerations, most samples studied lie somewhere between these two extremes. Decomposition may occur in competition with the volatilization and it becomes necessary to ensure that the peaks observed in the mass spectrum are the products of decomposition as opposed to a mass spectrum of the volatilized sample [20].

Figure 1 presents a schematic diagram of a DIP for introduction of solid samples into the ionization chamber via a vacuum lock system [21]. The probe may be inserted or removed from the MS without the system being vented to atmosphere. This probe is used in combination with a Bendix time-of-flight (TOF) mass spectrometer. A thermocouple used to heat the sample furnace is made of a 1 mm Pt/13% Rh–Pt wire and the furnace of high purity alumina. Sample crucibles (containing 1–5 mg of the sample compound) are of quartz tubing which can be linearly heated to approximately 800°C. Sample "blow out" in the ion source, due to pressure gradients within the sample, are prevented by use of a glass wool pad or frit. In this experiment Price et al. [21] investigated the solid state decomposition reactions of calcium oxalate. Characteristic ions *m/e* 28 (CO) and *m/e* 44 (CO_2) monitored for first and second stages of decomposition provided

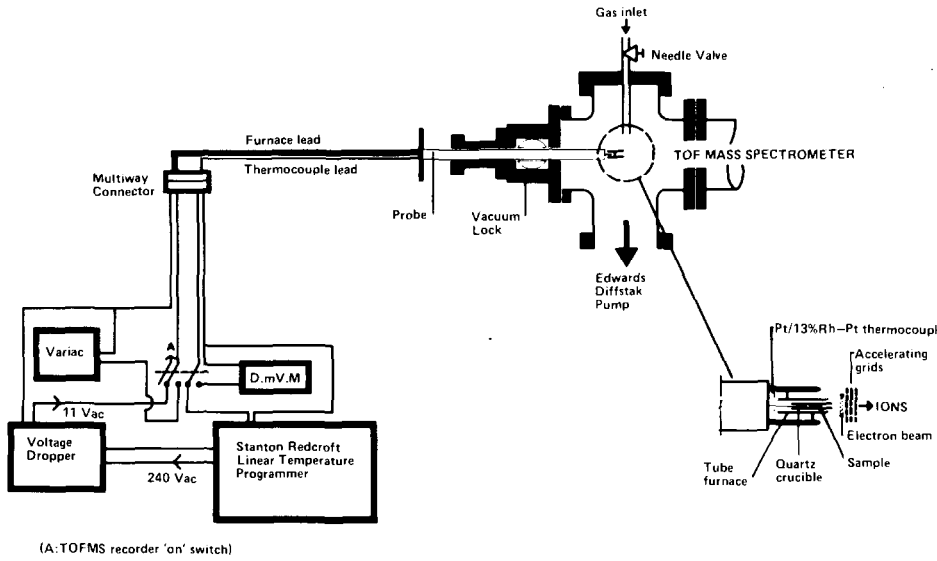

Fig. 1. Schematic diagram of a direct insertion probe into the source of a mass spectrometer. (Reproduced with permission from ref. 21.)

kinetic parameters concerning the two stages of decomposition of this material.

Smith [20] developed a method to alleviate the problems of volatilization that occur when programmed DIP is used. This method of helium atmosphere analysis (HAA) is compared with that of DIP (referred to by Smith [20] as programmed probe analysis (PPA)) using Zeise's salts. By the method of HAA the sample is heated in an inert atmosphere and a schematic diagram is given in Fig. 2. The furnace is connected to a jet separator for introduction of the volatiles to the MS. Figure 3 presents the observed difference in results of monitoring *trans*-dichloro(ethylene)–(pyridine)-

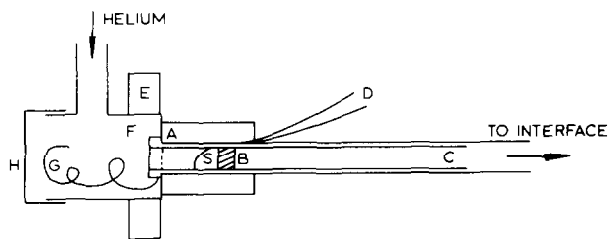

Fig. 2. Schematic view of the furnace used in helium atmosphere analysis (HAA). A, wire-wound heater; B, glass wool plug; C, open-ended melting point tube; D, thermocouple wires; E, transistor heat sink; F, silicone rubber ring; G, thin gold wire for removal of used sample; H, removable screw cap with O-ring; S, sample. (Reproduced with permission from ref. 20.)

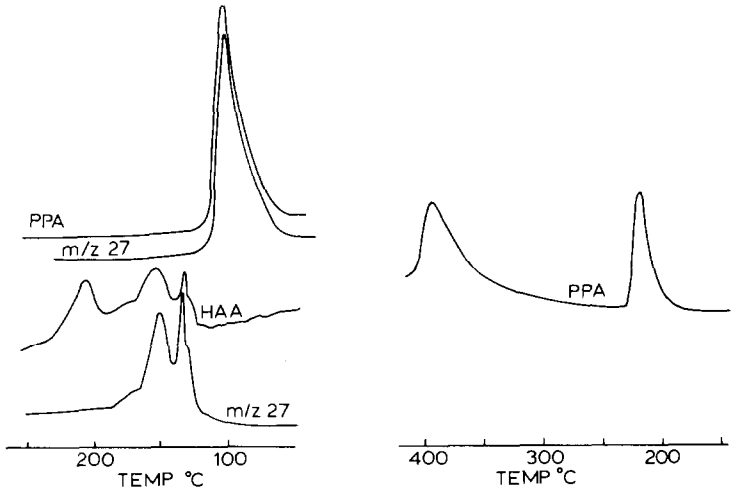

Fig. 3. Programmed probe analysis (PPA) and helium atmosphere analysis (HAA) for *trans*-dichloro(ethylene)–(pyridine)platinate(II). (Reproduced with permission from ref. 20.)

platinate(II) by these two methods. The total ion monitor by PPA demonstrates only one peak and using the selective ion monitor (SIM) only a mass of m/e 27 (possible ethylene evolution) was observable. However, the HAA output observed for the same compound is much more complex and reveals at least five processes occurring demonstrating much more information upon decomposition which is not obtainable by PPA. It should be pointed out that the HAA method did have the disadvantage (due to losses at the jet separator) of being approximately 1000 times less sensitive than the PPA technique.

DIP pyrolysis MS has also been contrasted with pyrolysis GCMS for the study of a styrene–isoprene copolymer [22]. A ribbon pyroprobe was interfaced to the GC inlet of a Finnigan 4000 MS and compared with a direct insertion ribbon pyroprobe. Pyrolysis was conducted in the same manner in which μg samples were heated to 650°C in five seconds. By DIP, characteristic isoprene (m/e 67) and styrene monomers (m/e 104) were noted along with a strong m/e 136 (isoprene dimer region) as demonstrated in Fig. 4B. However, pyrolysis GCMS revealed four major peaks, of which the third and fourth peaks observed in Fig. 4A were that of dimers of dipentene and dimethyl-vinylcyclohexene, respectively, therefore demonstrating the usefulness of prior chromatographic separation of volatiles [23].

DIP-MS can be heated at either slow or rapid rates and pyrolysis temperatures are usually below 400–500°C. Also, the evolved gases may have a fairly long residence time in the heating zone. When slow heating of a sample is required this may be accomplished by allowing the probe to be heated directly in the ion source, which avoids loss of evolved products by adsorption on transfer lines or chromatographic columns. This allows the use

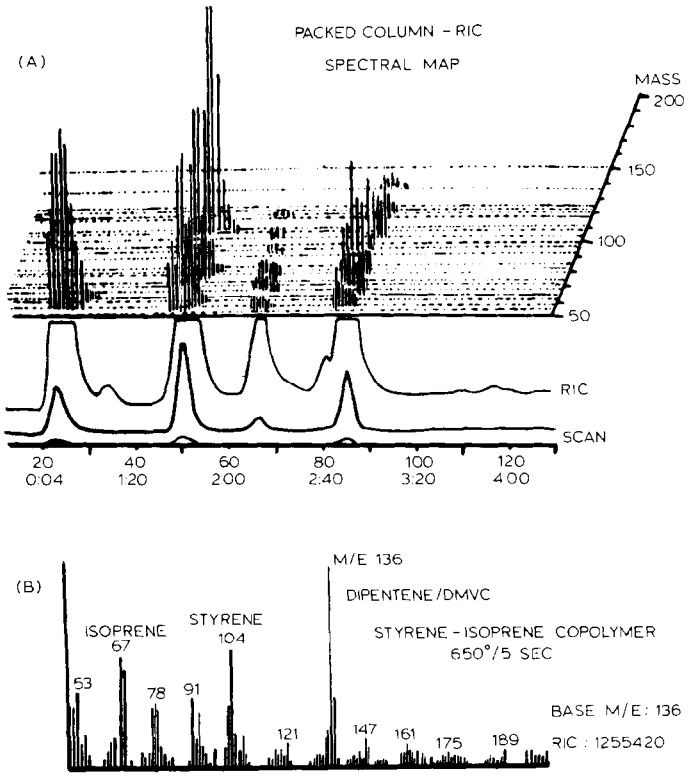

Fig. 4. (A), Pyrolysis GCMS of styrene–isoprene copolymer; (B), pyrolysis MS with direct insertion probe. (Reproduced with permission from ref. 22.)

of slow scanning magnetic sector instruments along with time resolution of the pyrolysis patterns. Since DIP inlets are available with most MS, little is needed in the way of complicated specialized equipment. Disadvantages of this technique include charring of samples due to slow heating rates and excessive contamination of the ion source which affects long-term reproducibility and increased down time for cleaning procedures. Due to the long residence time of the evolved products in the heating zone, secondary pyrolysis reactions may occur; however, ionization at low electron voltages (10–20 eV) minimizes secondary ion reactions and produce a less complex spectra with a large percentage of M^+ ions in the pyrogram [6].

There have been a number of applications of DIP pyrolysis MS and pyrolysis GCMS in different fields of chemistry since 1970. Beech and Lintonbon [24] studied the temperature dependence of mass spectra of some metal complexes of 2,4-pentanedione while Tang [25] has observed the solid-state decomposition of lead(II) dinitroresorcinate. Udupa [26] and Bell et al. [27] have studied the thermal decomposition of a number of organic compounds such as piperzinium diperchlorate and bigunide. Pyrolysis of cellulose and derivatives have also been investigated [28,29]. A temperature

programmed DIP was used to study and estimate primary pyrolysis products of unmodified and flame retardant cotton cellulose [28]. Pyrolysis GCMS has also been applied for determination of decomposition mechanisms of a number of organometallic compounds such as bis(diethyldithiocarbamato)-diphenyl–tin(IV) [30], tetrabis(diethyldithiocarbamato)–tin(IV) [31] and di-halotin(IV)–bis(diethyldithiocarbamate) [32] while others have applied the technique to the pyrolysis studies of polymers such as polyethylene [33], polyvinylchloride [34] and aromatic polyesters [35]. Reiner et al. [36] have used this method for differentiation of normal human cells. Differences in the qualitative and quantitative chemistry of human tissues such as kidney, spleen, liver and brain were noted.

Filament pyrolysis MS was first developed by Levy in 1963 [37], followed by development of Curie-point pyrolysis techniques in 1965 by Simon and Giacobbo [38]. Filament pyrolysis involves the heating of a sample deposited on a filament by galvanic current, whereas the Curie-point techniques involve heating a ferromagnetic filament by a high frequency coil. Curie-point pyrolysis MS possesses the advantages of low cost per filament and the ability to process hundreds of samples with maximum reproducibility for fingerprinting under controlled conditions.

Figure 5 presents a diagram of a Curie-point pyrolyzer quadrupole mass spectrometer system [39]. The pyrolysis reactor is connected to a three layered gold expansion chamber that opens to an electron impact ion source; the entire system is enclosed in a differentially pumped oil diffusion system. A quartz reaction vessel is connected to the steel probe via a polytetrafluoro-ethylene (PTFE) holder which contains the ferromagnetic wire with sample. The sample is positioned approximately half way into the high frequency coil which can be heated to pyrolysis temperature in 0.2–4 s. A signal averager allowed recording of repetitive mass scans as fast as 25 ms per scan. This system was utilized for the pyrolysis fingerprinting of different species of bacteria with a total analysis time of approximately 30 s.

Sample transfer can be a source of major problems for this instrumental method. Loss of pyrolysis products may occur before they reach the ionization zone, along with rearrangements and degradation. These products may form non-volatile charred materials which remain on the filaments, but this may be kept to a minimum by avoiding slow heating rates. Also, some pyrolyzed material may condense on the walls of the reaction vessels or transfer lines; this, however, can be overcome to an extent by heating the walls to a point above condensation but may still allow thermal degradation [6]. Figure 5 also contains a schematic diagram of a Curie-point wire-reaction tube assembly which is located within a high frequency coil. This glass reaction vessel serves to trap non-volatile products which may contaminate the MS source and produces a forward oriented beam of volatile products which enter the ion source or expansion chamber to obtain maximum signal intensity [6].

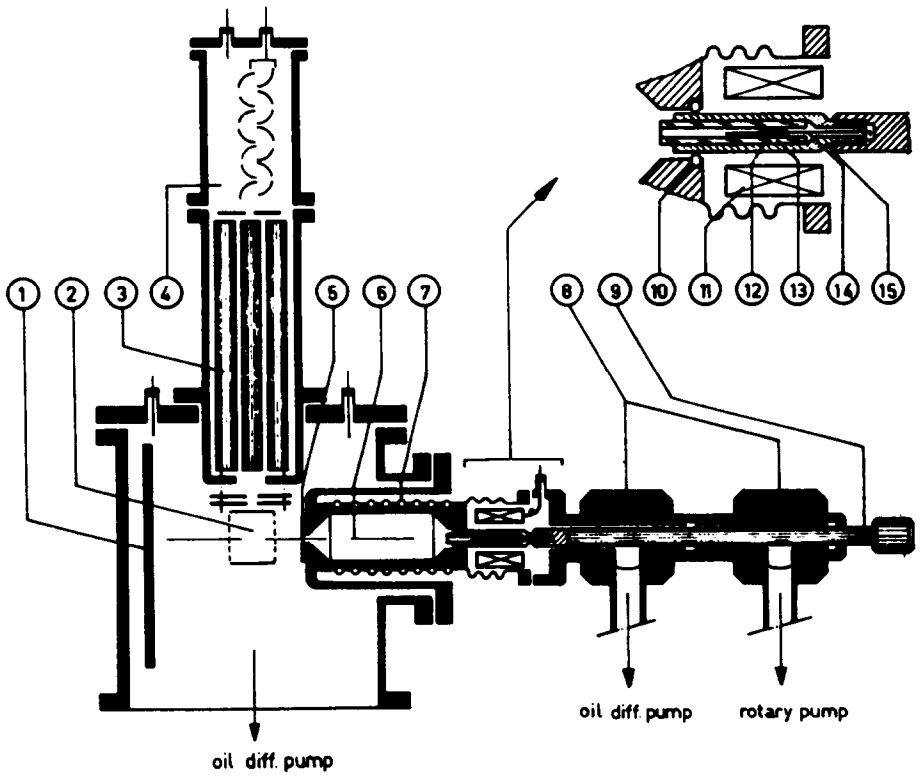

Fig. 5. Curie-point pyrolyzer quadrupole mass spectrometer system. 1, liquid N_2-cooled brass screen; 2, electron impact ionization cage; 3, quadrupole rods; 4, electron multiplier; 5, gold diaphragm with central 0.4 mm O pinhole; 6, expansion chamber (gold coated); 7, heating element; 8, three-way metal ball valves; 9, sample probe; 10, viton O-ring; 11, hf-coil; 12, sample region; 13, quartz reaction chamber; 14, ferromagnetic pyrolysis wire; 15, PTFE reaction tube holder. (Reproduced with permission from ref. 39.)

Figure 6 represents a diagram of an expansion chamber used for Curie-point pyrolysis MS. This chamber is heated to approximately 150°C and is composed of inert walls of gold-coated metal or quartz which vents into an ion source cooled by a liquid nitrogen trap. The chamber helps to keep degradation of pyrolyzed materials to a minimum and contributes tremendously to keeping ion source contamination to a minimum. It also allows a large number of mass scans to be made in order to obtain a representative averaged mass spectrum of the volatile products. Meuzelaar [6,40] has reported that as many as 1000 pyrolyses can be performed before ion source and inlet cleaning are needed.

Figure 7 represents an automated version of Fig. 6. This Curie-point pyrolysis MS is completely automated and has been applied for analysis and differentiation of bacterial products [6,41]. If the expansion chamber is used, increased scanning time is required per spectrum due to the longer residence time of the pyrolysate in the chamber. However, with removal of the

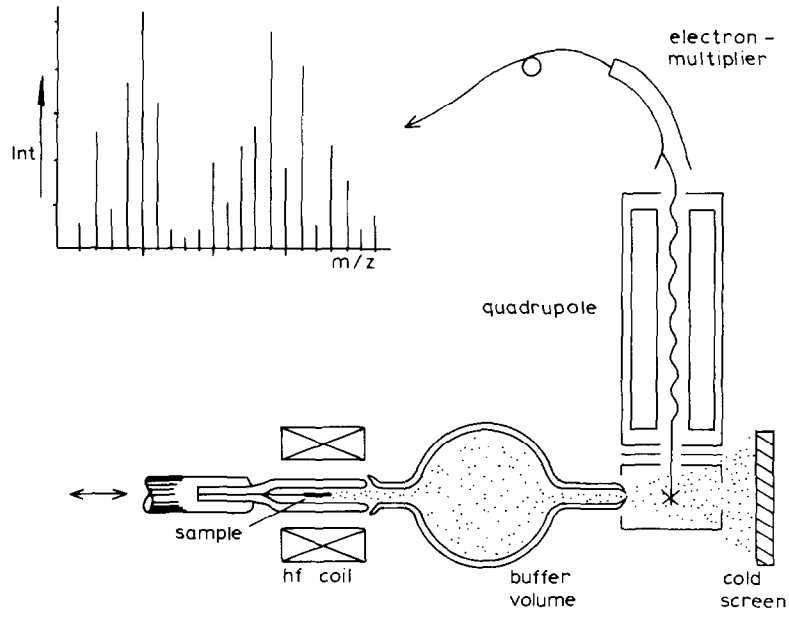

Fig. 6. Schematic representation of the pyrolysis reactor, expansion chamber, ion source region and quadrupole mass filter. (Reproduced with permission from ref. 6.)

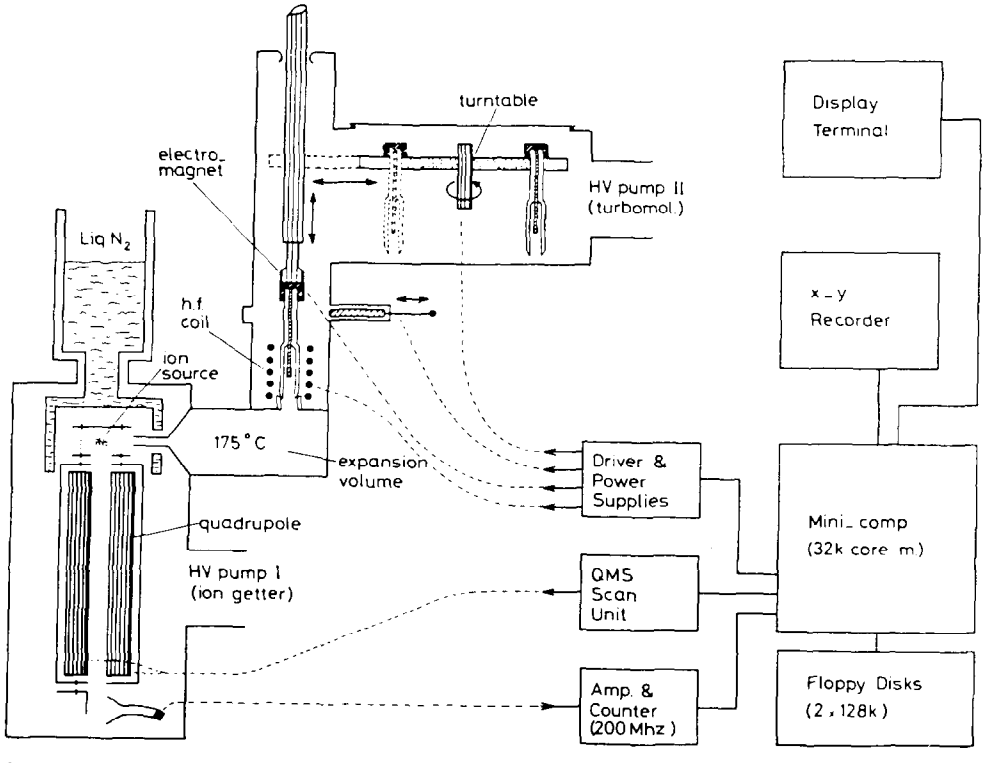

Fig. 7. Schematic diagram of an automated Curie-point pyrolysis MS system. (Reproduced with permission from ref. 6.)

expansion chamber, mass ranges up to m/e 800 may be required if information is to be obtained from large pyrolyzed materials [6,41].

Curie-point pyrolysis MS equipment has undergone many changes since its introduction to the scientific community in 1965. Advances have been made in speed of operation, such as data processing by computerization [42], high-speed ion counting [41] and interlaboratory standardization of pyrolysis MS methodologies [40], such as the availability of standard reference materials and spectra. For an excellent review of this subject the reader is referred to Meuzelaar et al. [6].

Field ionization (FI) and desorption (FD) MS methods have also been applied for identification of complex materials. These ionization techniques yield minimal fragmentation with enhanced molecular ion intensities and have been applied for analysis of complex biomaterials such as bacterial pyrolysis products [43]. Carsen and Egsgaard [44] have applied flash vacuum thermolysis in combination with FI-MS for the study of gas phase thermolytic reactions. Figures 8 and 9 illustrate the thermolysis unit and as combined with MS for use in their experimentation. The thermolysis unit contains a Curie-point pyrolyzator connected to a line-of-sight inlet system. Pyrolyzed products move directly into the ion source of a Varian MAT CH5-D magnetic sector–electric sector instrument with EI/FI/FD ion source (the field ion emitter consisted of a 10 μm tungsten wire activated by benzonitrile vapor). Collision activated mass spectra were obtained via introduction of helium gas by a needle valve at 10 G. Studying the formation of bimolecular reactions of *tert*-butoxy radicals into di-*tert* butyl peroxide, it

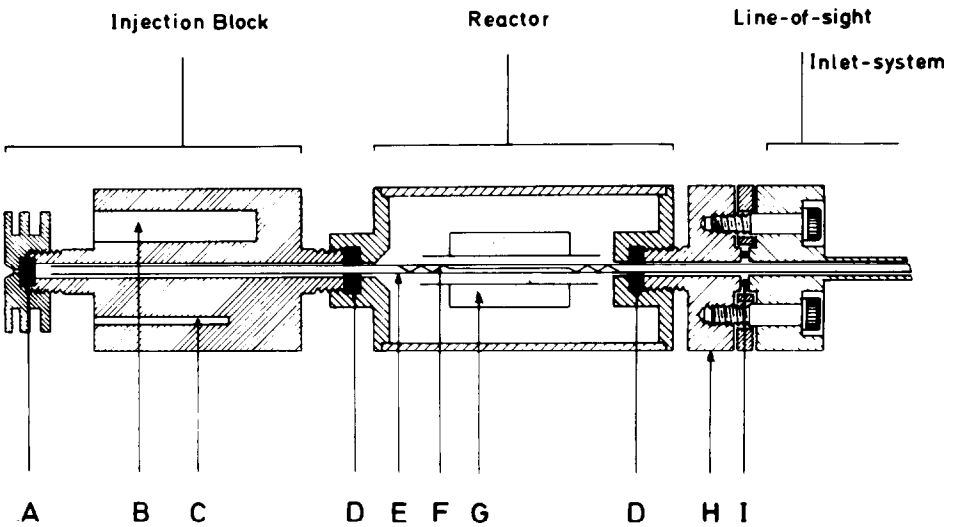

Fig. 8. Thermolysis unit. A, Septum; B, injection block heater; C, thermocouple for temperature readout; D, rubber washer; E, quartz lining tube; F, ferromagnetic wire; G, high frequency induction coil; H, adapter flange; I, gold wire sealing. (Reproduced with permission from ref. 44.)

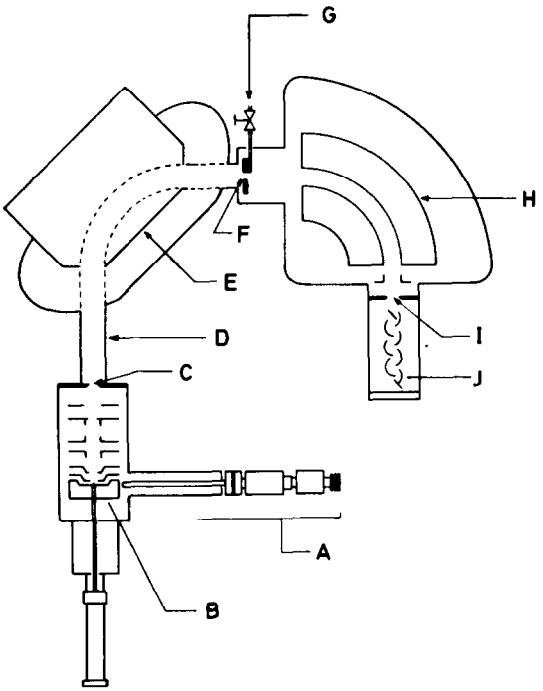

Fig. 9. Thermolysis unit–mass spectrometer set-up. A, Thermolysis unit; B, EI/FI/FD ion source; C, entrance slit; D, analyzer tube; E, magnetic sector; F, intermediate focus slit; G, needle valve; H, electric sector; I, collector slit; J, detector. (Reproduced with permission from ref. 44.)

was found that < 1% of the recombination was found by the FI-MS method. This particular technique offered advantages of studying very complex reaction product mixtures and FI gives rise to molecular ions with few fragmented ions of unstable substances. This particular paper demonstrated the superiority of FI over EI at 70 eV, due to the fact that several fragments were formed with EI of which the M^+ were not observable (Fig. 10 [44]) of trimethylsilyl-thionocarboxylate at 1043 K.

FI-MS in general does not provide much, if any, structural information due to the lack of fragmentation. However, the additional recording of collision activation (CA) MS of single FI molecules can supply this data. Figure 11 represents an example of the complementation of FI and CAMS with 5-phenyl-1,2,3-thiatriazole [44]. The FI-MS spectra without thermolysis and following thermolysis at 1043 K are represented along with CAMS spectra of the thermolysate. The molecular ion of m/e 103 is observable and the CAMS is in agreement with the known thermal decomposition of the molecule in question [44]. Others have also used combined FI-MS with complementary CAMS or single field ionized molecules [45–47] without flash vacuum thermolysis.

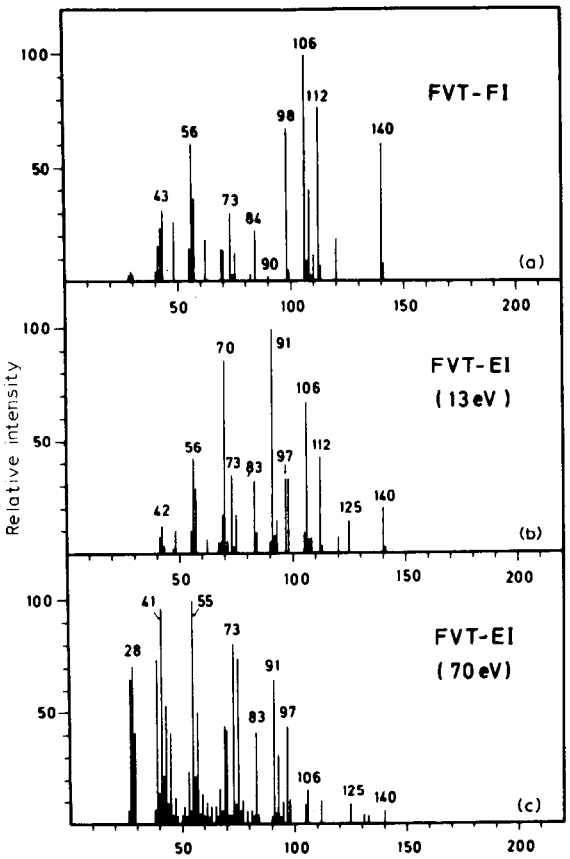

Fig. 10. FI-MS, 13 eV EI-MS and 70 eV EI-MS spectra obtained following flash vacuum thermolysis of trimethylsilyl-thionocarboxylate at 1043 K. The compound is totally degraded at this temperature and no molecular ion (M^{+} 246) is observed. (Reproduced with permission from ref. 44.)

The type of ionization mode used can greatly affect the generation of useable mass spectra. EI has mainly been the method used (low voltage 13–17 eV) for Curie-point pyrolysis MS. This ionization method provides production of M^{+} with long term reproducibility. Also, EI is readily obtainable with most MS whereas other techniques of chemical ionization (CI) and FI are not, or may require added expense and complicated equipment. CI is excellent for providing M^{+} of samples in low concentrations and provides for selectivity of ionization of chemical moieties with selection of specific reagent gases [48]. However, this has limited its use due to its ability to modify the chemical composition of the volatiles. FI has selected applications as previously discussed [44]. However, the production of polar compounds from the emitter surface can change the character of the ions, therefore limiting the use of this ionization mode [49].

Schulten et al. [43] have applied FD pyrolysis MS to the analysis of deoxyribonucleic acid (DNA). High resolution FD pyrolysis mass spectra

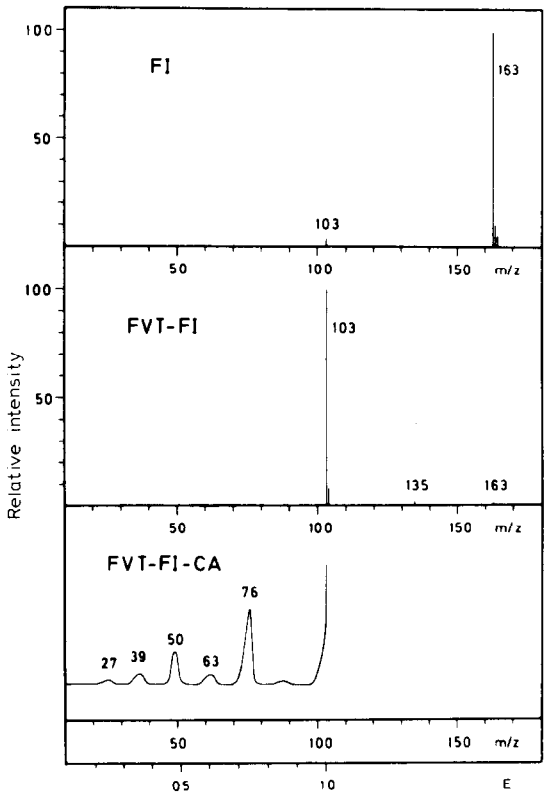

Fig. 11. FI-MS spectra of 5-phenyl-1,2,3,4-thiatriazole without thermolysis, following thermolysis at 1043 K and CA-MS spectrum of the thermolysate with $m/e = 103$. (Reproduced with permission from ref. 44.)

were obtained with a CEC 21-110B MS with a resolution of 30000 by photographic detection. DNA was suspended on a tungsten wire and heated with a 0–80 mA current over a period of 6 min. The spectra yielded no ions below m/e 112 and a relatively high abundance of ions in the mass range of m/e 200–400. Mass spectra revealed the presence of intense $(M + 1)^+$ ions for the five bases of adenine, guanine, cytsine, thymine and methylcytosine of herring DNA; some intact dinucleotide ions were also observable.

Knudsen cells have also been applied for EGA-MS [50–52]. Hirayama et al. [53] have analyzed the mass spectra of high temperature vapors on a Bendix time-of-flight MS with a Knudsen cell attachment. Various barium tungstates (300 mg) were loaded into the sample cell, with cell orifice diameters of 0.76–1.27 mm, and radiantly heated to 850°C. The cell was subsequently heated by electron bombardment and scanned via an oscilloscope while the electron accelerating energy was varied from 20–30 eV. In the study it was noted that the dominant vapor species over these mixed oxides was BaO (g) and that BaO was formed by the following solid state

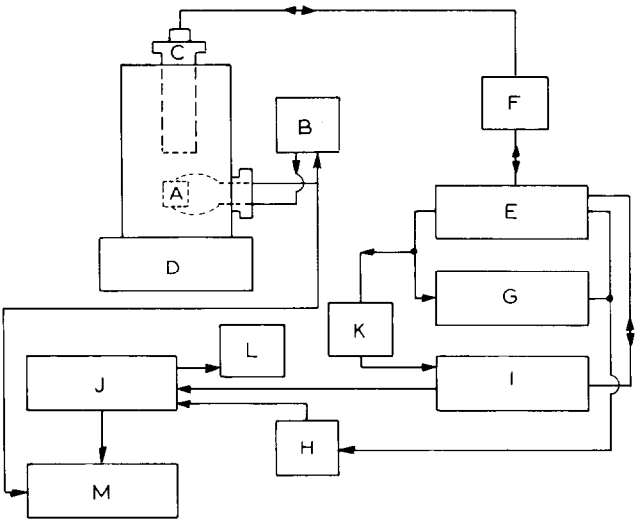

Fig. 12. Block diagram of EGA apparatus. A, furnace, B, furnace controller; C, quadrupole mass spectrometer head; D turbomolecular pump; E, control unit mass spectrometer; F, unit mass spectrometer; G, scope; H, relay; I, MS programmer; J, integrator; K, voltage divider; L, teletype; M, recorder. (Reproduced with permission from ref. 54.)

dissociation reaction

$$Ba_3WO_6(c) \rightarrow 2\ BaO(c) + BaWO_4(liq)$$

Evolution of gases from furnaces has also been analyzed by MS. Gallagher [54] developed an EGA system which consists of a Mo furnace attached to a quadrupole mass spectrometer (Fig. 12). The furnace is connected to a thermocouple of Pt/Pt–10%Rh for low voltage current and inserted into the vacuum chamber via a connection port. The chamber is evacuated to approximately 10^{-8} Torr and the evolved gases leaked into the MS which has a scanning atomic mass range of 0–300 a.m.u. The output of the MS is proportional to the intensity of the mass peak and is monitored directly by an oscilloscope. Evolved gases can be studied either isothermally or as a function of temperature or time. Figure 13 represents these three techniques with $CaCO_3$ as the experimental sample. Figure 13a illustrates the monitoring of the evolution of CO_2 (m/e 44) as the sample is heated at 1600°C h^{-1} and Fig. 13b demonstrates the monitoring of evolution of CO_2 by making short mass scans (12 a.m.u.) while the sample is heated at 400°C h^{-1}. These short scans help eliminate instrumental drift which may occur when monitoring only one ion. The third method (Fig. 13c) utilizes a larger mass scan so that information may be gathered on changes that occur over wider mass ranges. A complete scan varies from 1–10 min and fewer points are obtained for each mass but an overall picture of the decomposition process is obtainable.

Gallagher and others [55–57] have monitored evolved gases from a number of inorganic compounds. The samples were heated in similar fur-

naces as previously described and the decomposition products of iron oxides [55], cobalt hardened gold-plated films [56], europium hexacyanoferrate(III) and ammonium europium hexacyanoferrate(II) observed [57]. Brown et al. [58] studied the evolution of gases from graphite and non-graphitic carbons

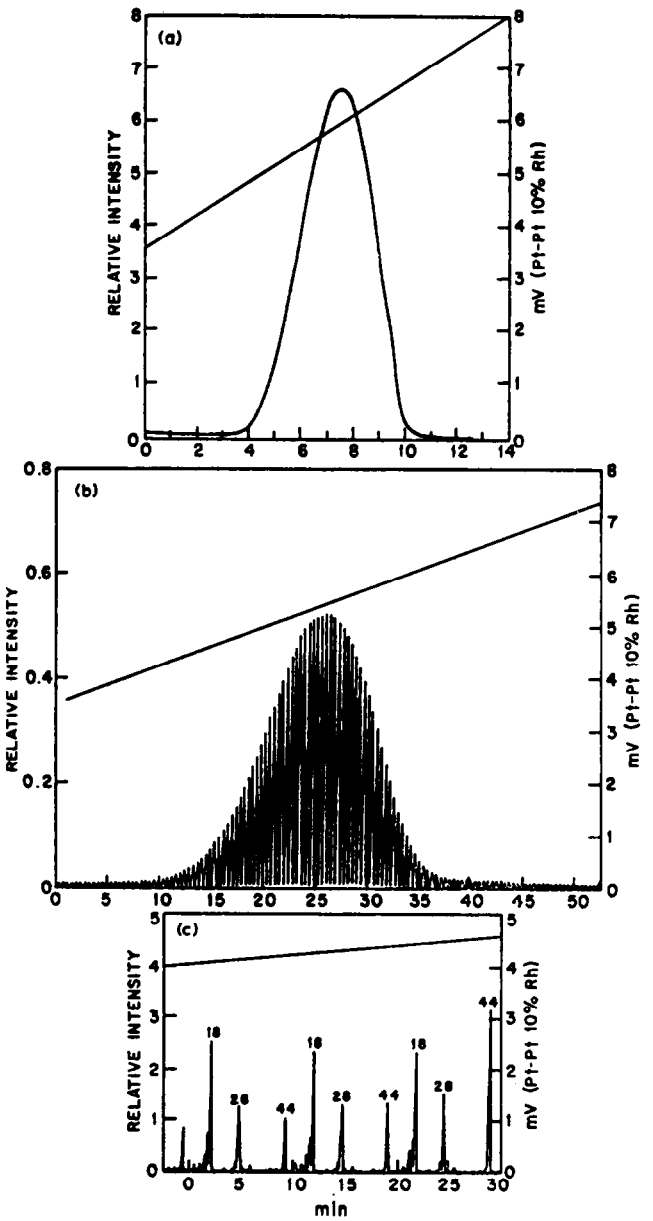

Fig. 13. Types of EGA curves and heating curves. (a) No scan, mass 44, 0.81 mg $CaCl_3$, 1600°C h^{-1}. (b) Short scan, mass 44, 0.79 mg $CaCO_3$, 400°C h^{-1}. (c) Long scan, 0–45 a.m.u., 0.54 mg $CaCO_3$, 100°C h^{-1}. (Reproduced with permission from ref. 54.)

by heating the samples in a furnace before introduction via a leak into the ion source, while Sakamoto [59] studied the volatile products formed from poly(methylmethacrylate) by a similar method. Pödör and Bertoti [60] have made similar studies of the reaction of γ-alumina oxide and carbon tetrachloride. A quartz microreactor was heated up to 900 K and the products observed by a quadrupole MS; it was noted that a surface reaction occurs at approximately 400 K with detection of the formation of products of $COCl_2$, CO_2 and Cl_2. At 600 K the volatilization of γ-alumina oxide was noted via the formation of $AlCl_3$.

(ii) Laser ionization and LAMMA methods

Various laser systems have been used in MS ion sources but have suffered in general from lack of speed, sensitivity or limited mass ranges [61–63]. Regardless of these limitations, earlier experiments demonstrated the potential of laser techniques. The various modes of laser instrumentation have been reviewed previously by Comzemius and Capellen [64].

Laser volatilization by ionization is not a well understood topic. It is generally believed (except in a few instances) that the wavelength of the laser is not as much of an important factor as is the duration and shape of the laser pulse [64]. The ratio of ions to neutral molecules is considered to be the ionization efficiency, which varies with the laser power density. An ionization efficiency of 10^{-5} or less is generated with a laser power density $< 10^8$ W cm^{-2} whereas power densities $> 10^9$–10^{10} W cm^{-2} produce ionization efficiencies in the range of 0.01–0.10 [63].

The earliest studies concerning laser pyrolysis were performed by Vastola et al. [65] and Joy et al. [66]. These investigators utilized a TOF-MS in combination with a ruby laser for analysis of coal samples. Karn et al. [67] described a laser MS method utilizing a combination of a ruby and CO_2 laser for pyrolysis of coal samples and analyzed by high resolution MS. Rhodes et al. [68] have used excimer laser-induced multiphoton ionization for ion generation in capillary GCMS for analysis of polyaromatic hydrocarbons. This laser technique is capable of being a highly efficient soft ionization method at low laser intensities while producing considerable fragmentation at higher intensities. A block diagram of this instrument can be seen in Fig. 14. The photon source was operated with either KrF or XeCl as lasing media ($\lambda = 2485$ and 3080 Å) with pulses of 10 ns duration. After a fraction of the beam was passed through a rectangular aperture it was focused into the ionization region of the MS where the chromatographic effluent entered the source. A TOF-MS with a 61 cm flight tube was utilized for analysis and the data stored via an Apple II microcomputer. Figure 15 presents an example of the sensitivity observed with this instrument. The selected ion chromatograms of naphthalene are 5 pg, 2.5 pg and 500 fg, respectively. Figure 16 represents the comparison of a flame ionization

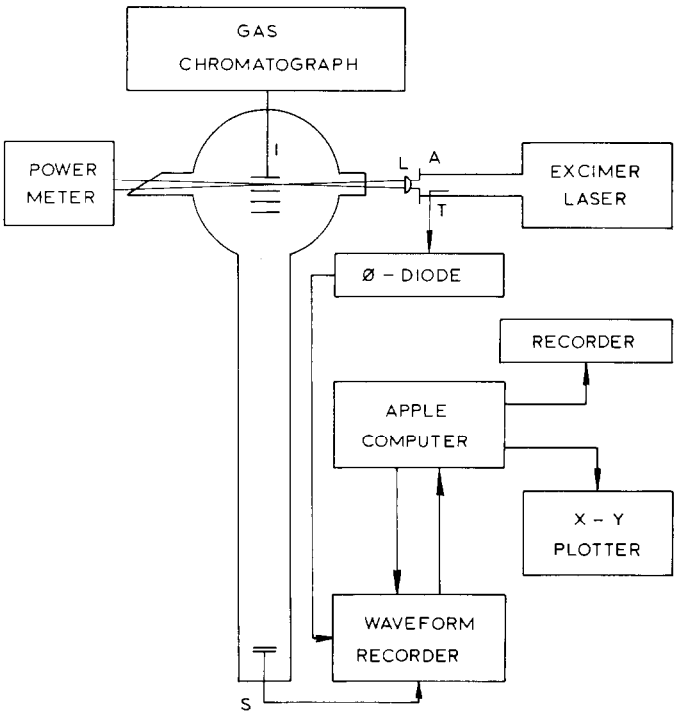

Fig. 14. Block diagram of the multiphoton ionization GCMS apparatus. (Reproduced with permission from ref. 68.)

detector with that of the laser multiphoton ionization GCMS. In Fig. 16 A the FID spectra of naphthalene, biphenyl, acenaphthene, fluorene, anthracene and pyrene are observed whereas Fig. 16C represents the ion monitoring of masses *m/e* 128, 154, 154 and 166 (naphthalene, biphenyl, acenaphthalene and fluorene, respectively) following ionization by the laser. The

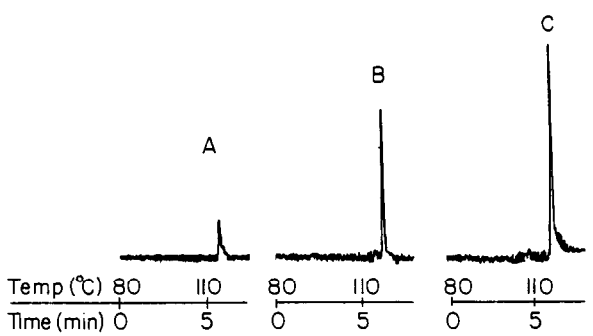

Fig. 15. Selected ion chromatograms demonstrating detection sensitivity for naphthalene: A = 500 fg; B = 2.5 pg; C = 5 pg. (Reproduced with permission from ref. 68.)

limit of detection for these compounds ranged in the neighborhood of 0.20–5.00 pg for the compounds observed [68].

Others have applied various laser techniques for EGA-MS. Schulten et al.

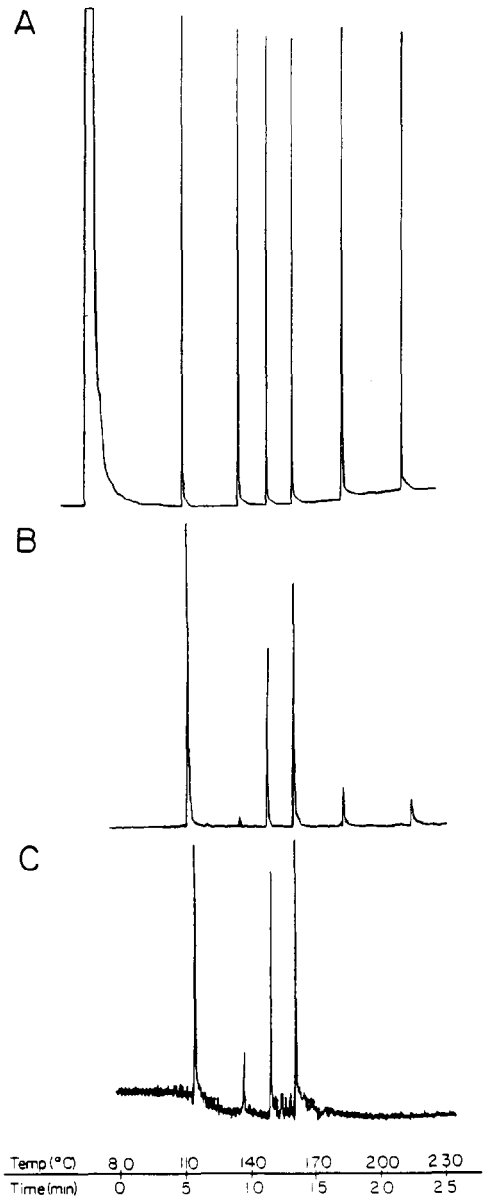

Fig. 16. Chromatograms of a polyaromatic hydrocarbon mixture: A, 30 ng each of naphthalene, biphenyl, acenaphthalene, fluorene, anthracene and pyrene with a flame ionization detector; B, 500 pg of the same compounds with laser ionization detector, monitoring total mass-integrated ion yield; C, 20 pg of some compounds with laser ionization detector selectively monitoring masses m/e 128, 154 and 166 only. (Reproduced with permission from ref. 68.)

[69] applied laser-assisted field desorption MS for molecular weight determination, structural elucidation and purity control of inorganic and organometallic compounds. Others have applied CO_2 lasers to the analysis of synthetic polymers [70] and nucleic acids [71].

Since 1972 the field of laser pyrolysis MS has seen the development of a new technique referred to as laser microprobe mass analyzer (LAMMA) [72]. The method was originally developed for application of measurement of trace metals and electrolytes in cellular fluids but its applications have now extended into the realms of polymer, inorganic and organometallic chemistry. Commerical LAMMA instruments (Leybold-Heraeus LAMMA-500) have recently been introduced and represent a significant breakthrough in laser MS [73]. Lum [74] has recently described a LAMMA technique which enables the overall course of the polymer decomposition process to be followed directly. A schematic diagram of this apparatus can be seen in Fig. 17. A low power argon-ion laser ($\lambda = 514.5$ nm) was used to probe the samples with beam intensities of 10–1000 W cm^{-2}. A sample cell was directly coupled to the inlet of the MS and upon irradiation a plume of volatile products was generated at the polymer surface. The volatile products immediately formed a molecular beam which was ionized by 70 eV electron impact and analyzed by a quadrupole mass filter. Prior to ionization the

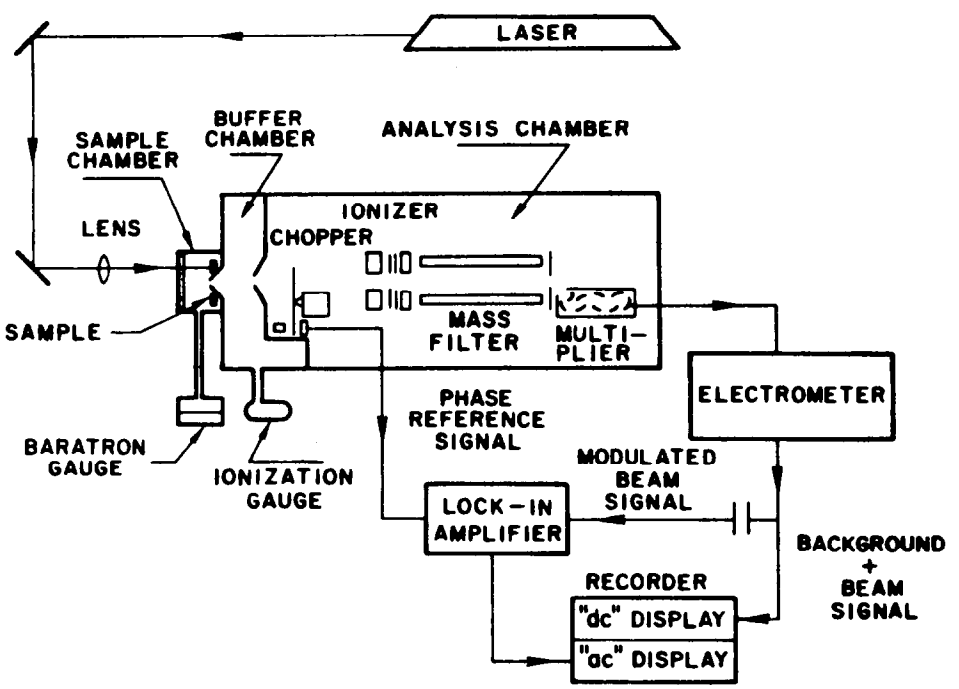

Fig. 17. Schematic diagram of laser microprobe mass analyzer–molecular beam apparatus. (Reproduced with permission from ref. 74.)

molecular beam was modulated with a mechanical chopper. The typical focussed laser beam produced a 400 μm hole with 3 mm depth. Figure 18 represents the modulated mass spectrum of the volatile pyrolysis products of polyvinylchloride, of which the dominant products were hydrogen chloride (*m/e* 35–38). Benzene (*m/e* 78) and toluene (*m/e* 91,92) were also observable, as were the products of naphthalene (*m/e* 28) and methylnaphthalene (*m/e* 142) which were not recorded on this spectra. This technique was also applied to the evolution profile of characteristic volatile products of polymers over irradiation time and for phase measurements of evolved products.

Schiller et al. [75] have applied LAMMA methods to the study of amino acids and peptides. Generally, quasi-molecular ions $(M-1)^-$ and $(M+1)^+$ were observed while non-aliphatic amino acids produced positive ion spectra. Vanderborgh and Jones [76] applied LAMMA methods to analysis of coal and shale samples and DeWalse et al. [77] have analyzed fiber surfaces for organic compounds; LAMMA methods have also been utilized for analysis of cobalamins [78]. Due to the differences in the positive and negative ion spectra structural charges could be related to this data. Balasanmugam and Hercules [79] have compared the quantitative aspects of LAMMA with that of HPLC of mixed benzalkonium chlorides. They found that the ratio of the positive ion spectra for the intact cation peaks related

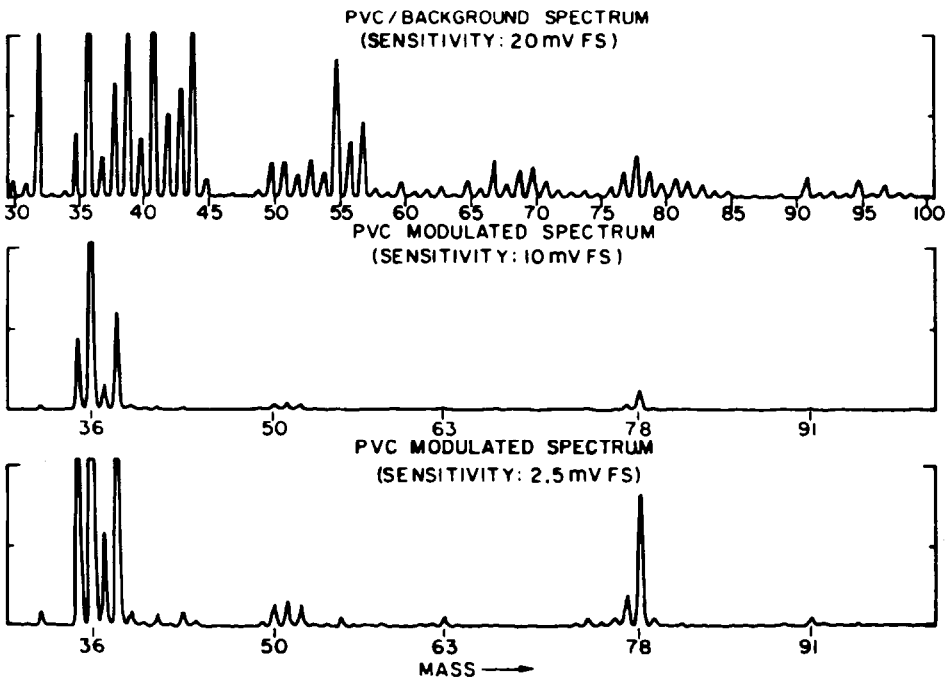

Fig. 18. Simultaneous "d.c." and modulated mass spectra from laser irradiated rigid PVC. (Reproduced with permission from ref. 74.)

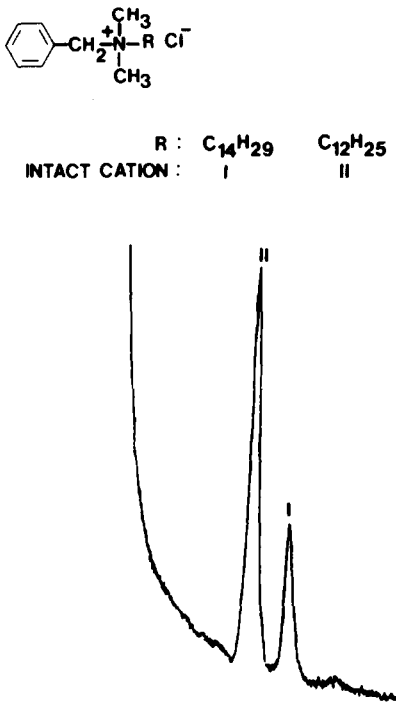

Fig. 19. HPLC separation of benzalkonium chloride mixture (I, II). (Reproduced with permission from ref. 79.)

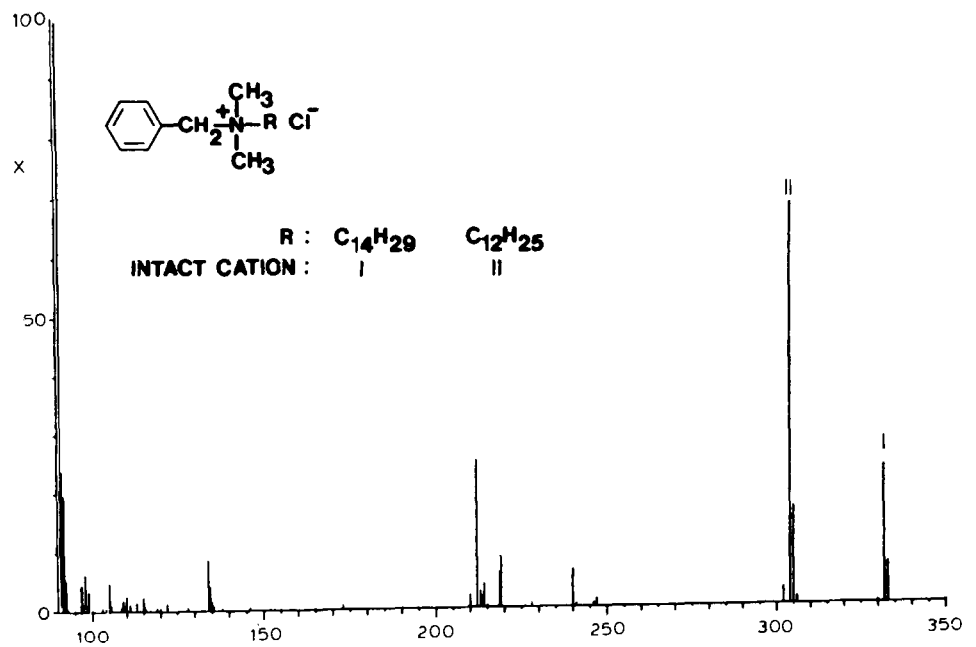

Fig. 20. Laser desorption mass spectrum of benzalkonium chloride mixture (I, II). (Reproduced with permission from ref. 79.)

significantly to the ratio of these compounds when separated by HPLC for quantitation, whithin an experimental error of $\pm 10\%$. Figures 19 and 20 demonstrate the HPLC separation and laser desorption mass spectra of these two compounds. The ratio of II : I for HPLC was found to be 3.0 and the ratio of II : I by the laser method was 2.9 ± 0.3, demonstrating the quantitative abilities of this method. Quantitative capabilities of this instrumentation have also been observed with a number of metals doped into epoxy films. Calibration curves for lithium and lead were linear over three decades of concentration and the absolute limits of detection were very impressive, with a detection limit for potassium of 1×10^{-20} g (or 150 potassium atoms) [63].

The unique advantage of laser and LAMMA instrumentation is its microprobe capabilities. This microprobe has provided mass spectral data for a number of medical and chemical uses. As examples, the laser microprobe has provided quantitative measurements on uranium content of single cells [80] and semiquantitative data of Na and K in bacterial cells [81]. Data of this nature has been useful in investigations of minute biological cellular processes such as the sodium pump and calcium transport systems.

(iii) Differential thermal analysis

DTA-MS was first reported in 1965 by Langer et al. [82] in which the furnace was replaced with a modified DTA cell which allowed stimultaneous DTA measurements along with gas analysis thermograms. This instrument was applied to analysis of triphenyltin hydroxide and $MgCl_2 \cdot 6\ H_2O$ decomposition reaction. Langer and co-workers [83,84] later modified this equipment for automation and applied this technique for studies involving trivinyltin hydroxide and cyclopentadienyl nickel chloride–triphenyl phosphine complexes. Others have coupled DTA with magnetic sector MS for the study of inorganic hydrates [85] and high resolution MS for investigations of thermal decomposition reactions of certain polymers [86]. Wendlandt et al. [87,88] modified an EGA-MS system to incorporate DTA; this system was utilized to identify the gaseous pyrolysis products of the decomposition of potassium methylsulfate.

All the investigations of DTA-MS described in the above paragraph occurred before 1970. Since that time few changes have occurred in the instrumentation required for these techniques and not a tremendous number of applications have been published. Langer and Brady [89] described their DTA-MS instrumentation with applications to analysis of inorganic, organic and polymeric compounds. Figure 21 is a schematic diagram of their original instrumentation described in 1969 [84] with the modified external DTA cell for mass spectral analysis (Fig. 22). The instrument consisted of a modified DuPont 900 thermal analyzer, a TOF mass spectrometer, scanning oscilloscope, frequency modulated magnetic tape recorder and an XY recorder; ten mass spectra could be recorded per second. Figure 22 represents the mod-

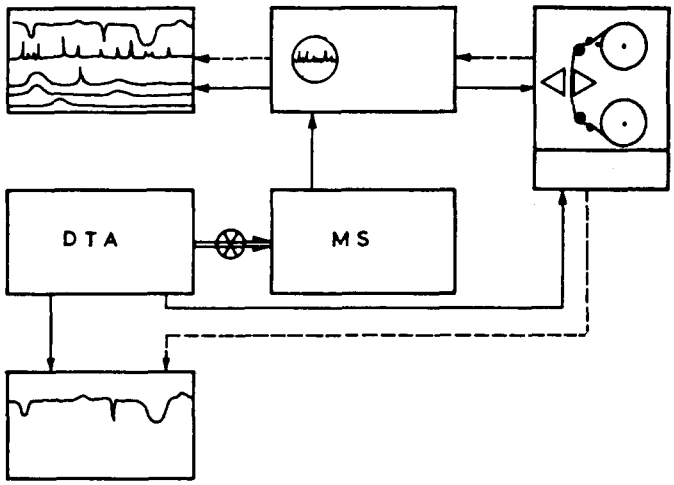

Fig. 21. Schematic diagram of mass spectrometer–differential thermal analysis system. (Reproduced with permission from ref. 89.)

ified external DTA cell whereas for internal operation with the MS the cell was miniaturized and secured onto the end of a probe which could be inserted into the ion source. The decomposition of the monohydrate of tetramine copper sulfate was studied with this instrument and in Fig. 23 the DTA thermogram of this material can be observed. It has been expected that there might be a stepwise release of ammonia until a final product of anhydrous copper sulfate was left if observed by DTA. However, when decomposed in an argon atmosphere and observed by MS (Fig. 24) it is noted that 2 moles of ammonia and water are released early in the degrada-

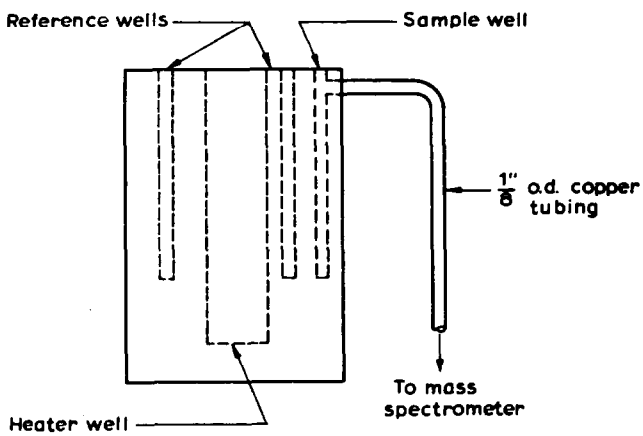

Fig. 22. External DTA cell modification for mass spectral analysis. (Reproduced with permission from ref. 89.)

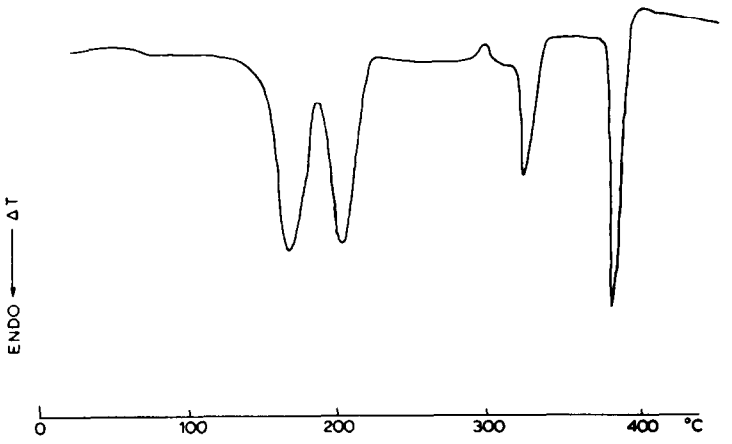

Fig. 23. Thermogram of the monohydrate of tetramine copper sulfate. (Reproduced with permission from ref. 89.)

tion followed by separate release of an additional mole of ammonia. The final decomposition step involves a redox reaction with formation of nitrogen, ammonia, water and sulfur dioxide [84].

Figures 25 and 26 demonstrate the different decomposition products of the same compound when observed in a vacuum. In Fig. 25 the sample is

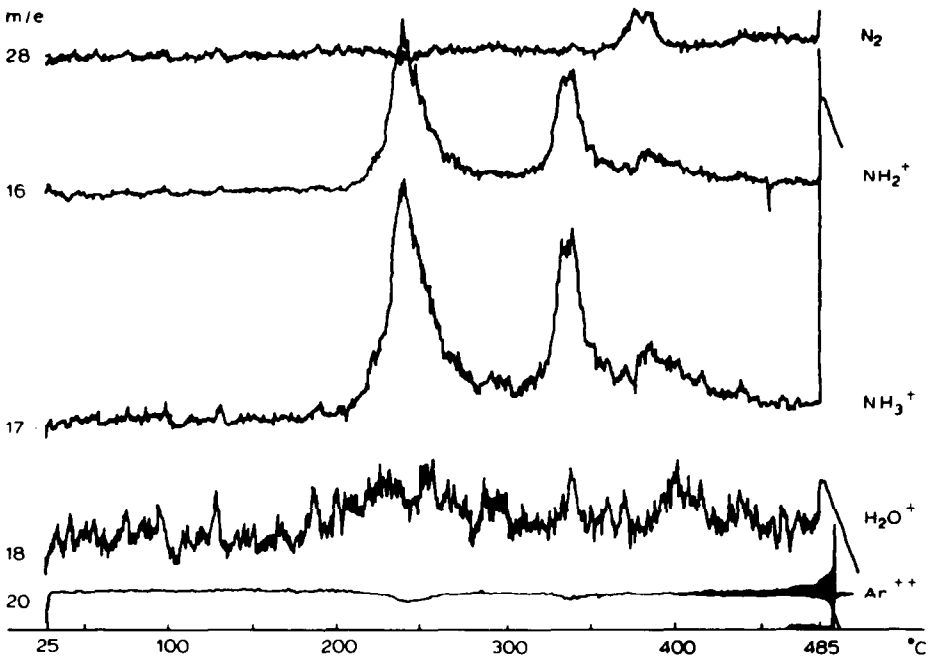

Fig. 24. Ion intensities vs. temperature for tetramine copper sulfate monohydrate decomposition in an argon atmosphere (external DTA cell). (Reproduced with permission from ref. 89.)

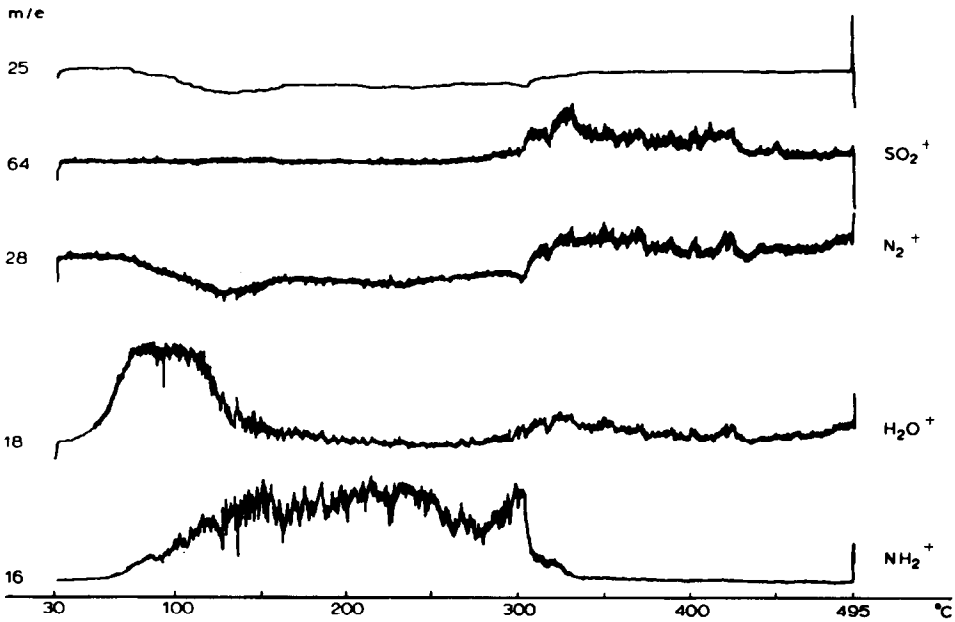

Fig. 25. Ion intensities vs. temperature for the tetramine copper sulfate monohydrate decomposition at 10^{-5} Torr (DTA cell inside MS), immediate heat. (Reproduced with permission from ref. 89.)

heated by the miniaturized DTA cell held inside the MS and two different reactions cause release of water and ammonia below 300°C. The release of water at room temperature indicates that it is very loosely held as a water of

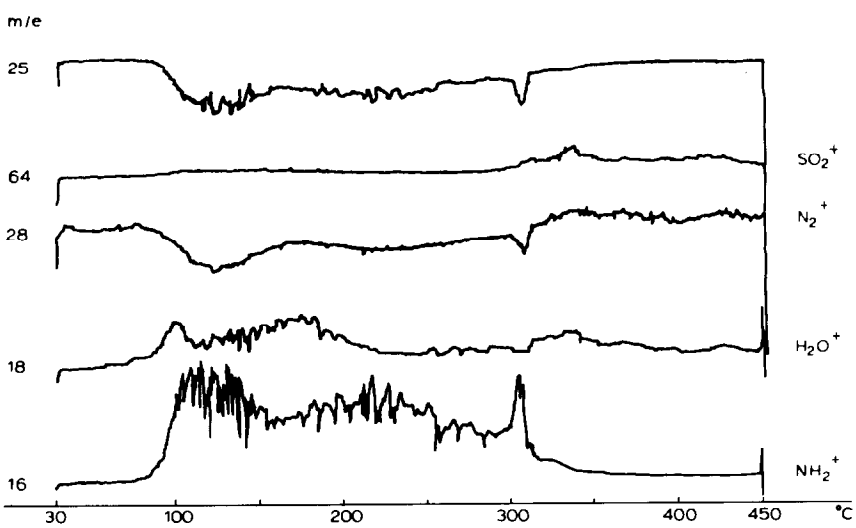

Fig. 26. Tetramine copper sulfate monohydrate decomposition inside MS after 24 h at 10^{-5} Torr. (Reproduced with permission from ref. 89.)

crystallization. Figure 26 confirms this finding in which the sample is held under vacuum for 24 h. Following analysis, little of the water of crystallization is observable by MS. Therefore, this example of combined DTA-MS demonstrates not only identification of decomposition products but also the mechanism by which it occurs and structural information about the molecule in question.

Dollimore et al. [90] have applied this combined technique to the decomposition studies of ammonium exchanged zirconium phosphates and

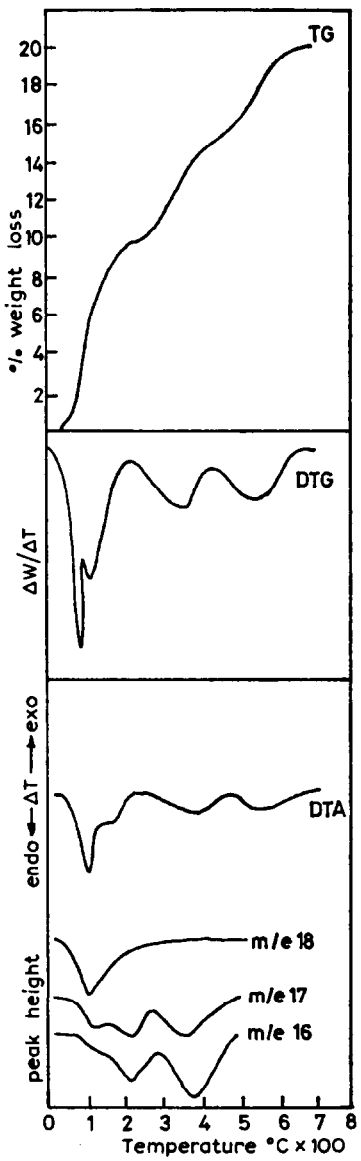

Fig. 27. Thermal and mass spectral analysis of α-zirconium bis(monohydrogen *ortho*-phosphate) monohydrate. (Reproduced with permission from ref. 90.)

zirconium arsenates. Figure 27 demonstrates the thermal and mass spectral analysis of α-zirconium bis(monohydrogen *ortho*-phosphate) monohydrate. The decomposition takes place in three stages in which the first stage involves loss of 1 mole of water and ammonia at 65°C followed by loss of 1 mole of ammonia (second stage). The final stage involves loss of 1 mole of water at 475°C due to the condensation of *ortho*-phosphate to pyrophosphate. This sequence is nicely demonstrated by the support of the TG, DTG and DTA curves and the mass analysis of ions m/e 16 and 18 for ammonia and water (m/e 17 is representative of isotopic contribution from both compounds).

(iv) Thermogravimetric analysis

TGA has enjoyed a more popular career of adaptation to mass spectrometers. The first direct coupling of a thermobalance to a TOF-MS was in 1968 by Zitomer [91] who studied thermal decomposition of polymers. Since that time a number of variations in TGA-MS have been published which were applied for different chemical systems. Gibson and Johnson [92] used TG-quadrupole MS for investigations concerning decomposition processes and identification of released volatile components of geological samples. This instrument was orginally developed by Wiedeman [93] in 1964 and was capable of operating temperatures up to 1600°C at a vacuum of approximately 2×10^{-6} Torr. Gibson [94] later added a data system to the above mentioned instrument and applied it to analysis of shale and lunar soil samples. Mol [95] coupled a Mettler Thermoanalyzer to a UTI 100 C precision mass analyzer by attaching a vacuum connector to the quartz furnace as seen in Fig. 28. Direct coupling to the furnace eliminates trapping problems and collecting fractions for analysis. At the end of each run the furnace had to be heated to 600–700°C for at least 2 h and the mass probe at 340°C to bake out the system. Polyurethanes were used as sample materials for demonstration of the usefulness of this technique for thermal analysis.

Chiu and Beattie [96] developed a technique for thermal evolution-differential trapping-MS for polymer characterization. This instrument combined a TG analyzer without using the balance mechanism and four U-shaped glass traps (three in series and one in a parallel arrangement, held at different temperatures) with the MS. As polymer samples were heated, the volatile products were trapped and later allowed to evolve into the ion source for identification. The use of thermal evolution of the samples was used to derive quantitative information on the basis of pressure change detection with Pirani gauges. Figure 29 represents the quantitative aspects of the Pirani gauge detection with Teflon 6 (polytetrafluoroethylene). This material completely depolymerizes to produce the monomer by first order kinetics. Thermal evolution was performed by heating at a rate of 10°C min^{-1} and a

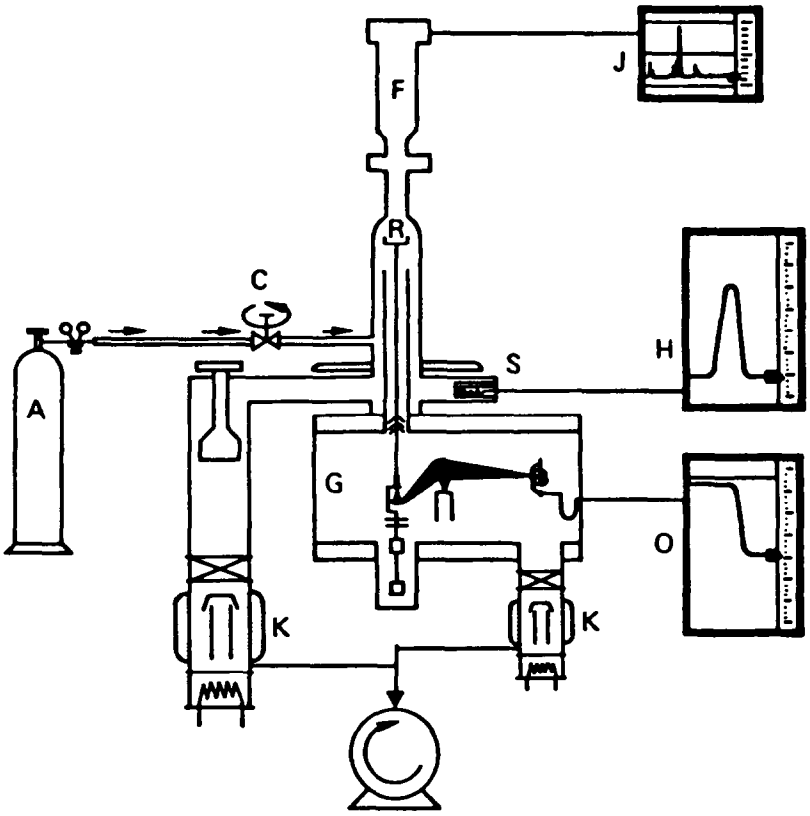

Fig. 28. Schematic diagram of a Mettler thermoanalyzer coupled to a UTI 100 C precision mass analyzer. (Reproduced with permission from ref. 95.)

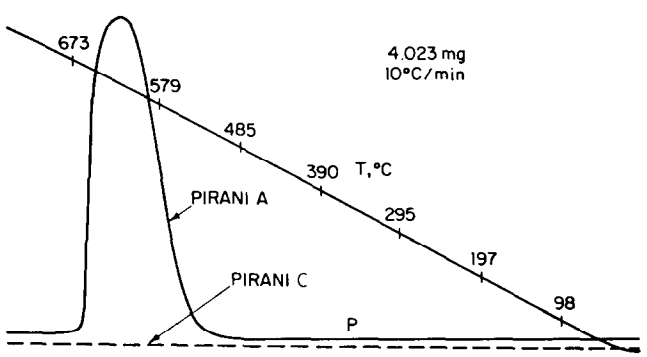

Fig. 29. Thermal evolution curves of Teflon 6. Sample weight, 4.023 mg; heating rate, 10°C min^{-1}; P, total pressure; T, sample temperature in °C. (Reproduced with permission from ref. 96.)

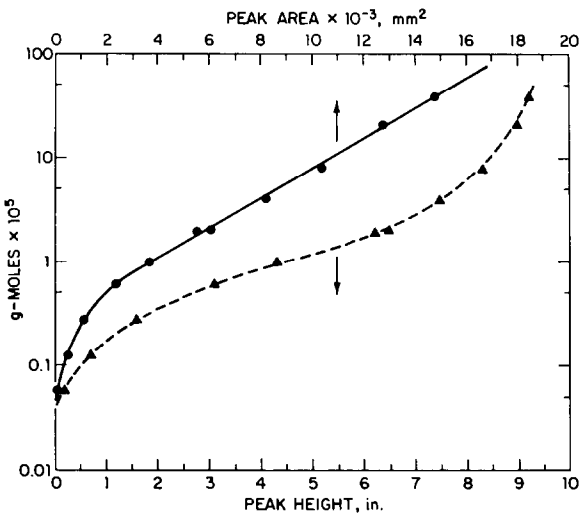

Fig. 30. Response of TFE. (Reproduced with permission from ref. 96.)

typical scan is presented in this figure. Pirani gauge A gave a single smooth evolution peak which was the total amount of sample originally tested. Gauge C did not detect any residual gas after trap II. Figure 30 presents the logarithm of moles of this polymer vs. both peak areas and heights; peak height demonstrating an S-shaped response to pressure, which correlated with the moles of volatile product. Peak areas are more linear (with the exception of small amounts of materials) thus suggesting the use of areas for quantitative determinations when gathering thermal evolution data. Baumgartner and Nachbaur [97] published data concerning simultaneous application of a thermobalance and a quadrupole MS with chemical ionization. Since chemical ionization has an advantage of avoiding some interference problems and reducing the fragmentation of evolved gases, it has the ability to be used to study quite complex reactions. Eppler and Selhofer [98] have addressed a number of problems that arise with the coupling of quadrupole MS with thermoanalyzers as well as the mechanical connection of these two techniques for combined use.

Chiu and Beattie [99] have described the coupling of a TGA with a quadrupole MS and applied the equipment to analysis of polymer volatiles. Figure 31 presents a schematic diagram of their instrumentation. A conditioner between the TG analyzer and MS is maintained at preselected temperatures to remove undesirable less volatile materials, prevent clogging of the microvalve inlet and MS contamination. Evolved gases are completely condensed in the liquid nitrogen trap and then thermally evaporated into the MS via the microvalve. According to the authors there is no dilution of the evolved samples when helium is used as carrier gas. This technique allows for total condensation followed by re-evolution of the gaseous vapors. The

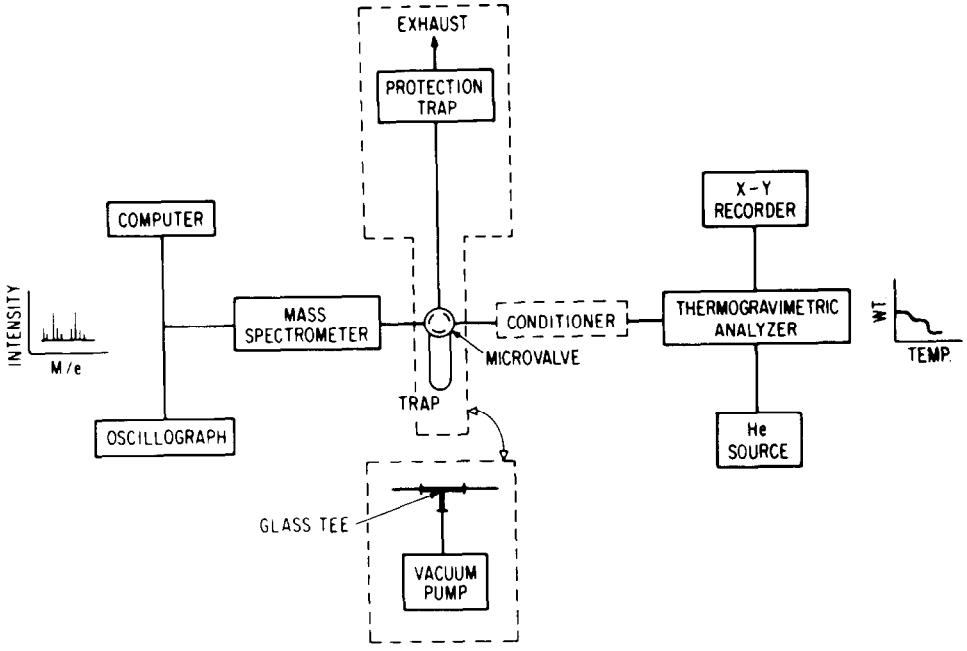

Fig. 31. Schematic diagram of TG–MS system. (Reproduced with permission from ref. 99.)

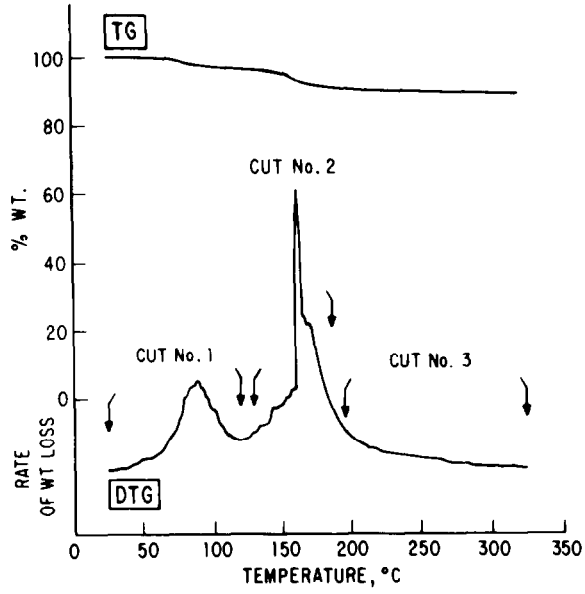

Fig. 32. TG of a polyimide prepreg. Sample weight, 25 mg; heating rate, 10°C min^{-1}; helium flow rate, 60 ml min^{-1}; sensitivity, 5.0 mg in^{-1} on Y and 0.2 mg in^{-1} on dY. (Reproduced with permission from ref. 99.)

system is also set up for continuous monitoring of the gaseous effluent by replacing the microvalve trap with a glass tee as shown in the figure. By proper control of the carrier gas flow and sample size, most organic vapors of interest can be allowed into the MS. Figure 32 demonstrates a thermogram of three weight loss steps of polyimide prepreg. As the samples evolve, mass spectra are recorded at cuts 1, 2 and 3 and are presented in Fig. 33. The representative mass spectra demonstrate the combinations of evolved products at each successive weight loss. For the continuous monitored mode, observe Figs. 34 and 35. This is the sample of polyimide prepreg of which the TG analyzer thermogram was presented in Fig. 33. Mass spectra were recorded every 2 min and are so numbered on the DTG curve. Water and ethanol, the two major components, are monitored by observing m/e 18 and 31, respectively, and their intensities are plotted as a function of tempera-

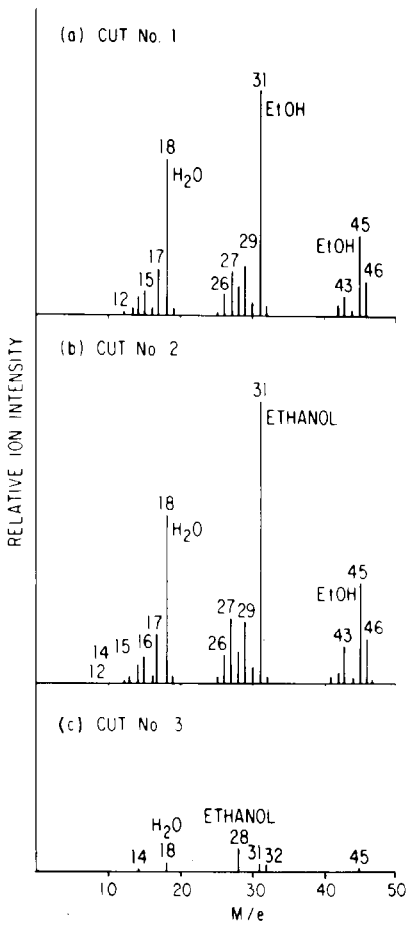

Fig. 33. MS spectra of volatile products from TG of a polyimide prepreg. (a), (b) and (c) are for weight loss cuts 1, 2 and 3 shown on the DTG curve. (Reproduced with permission from ref. 99.)

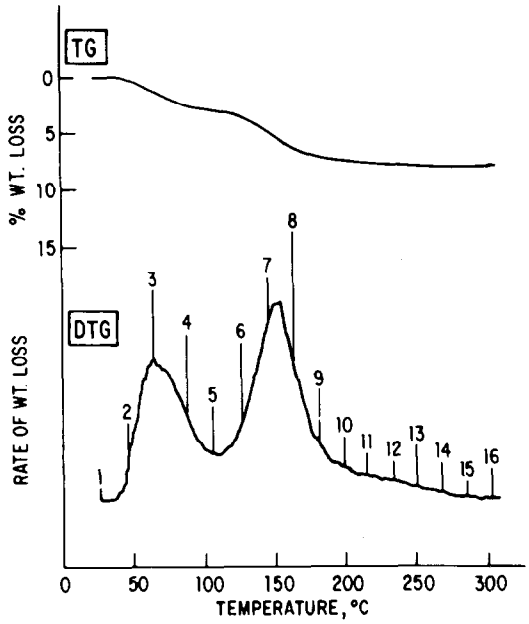

Fig. 34. TG of polyimide prepreg with continuous monitoring by MS. Sample weight, 76 mg; heating rate, 5°C min^{-1}; helium flow 60 ml min^{-1}; sensitivity, 5 mg in^{-1} on Y and 0.2 mg min^{-1} in on dY. (Reproduced with permission from ref. 99.)

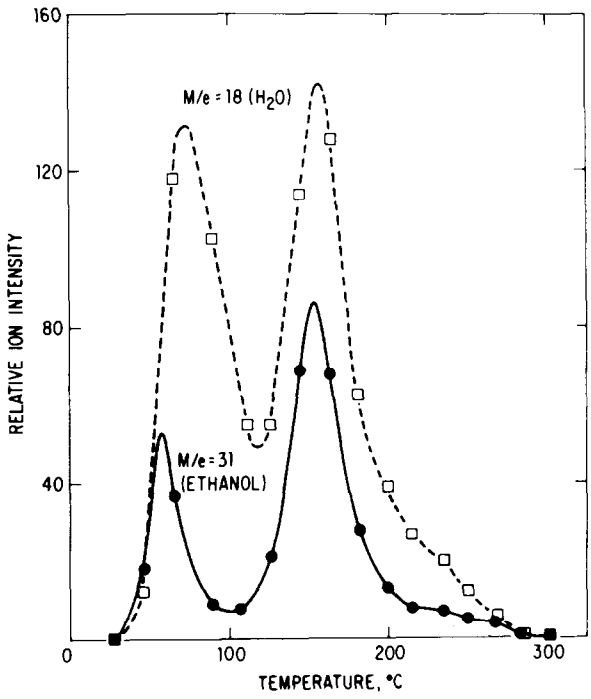

Fig. 35. Relative ion intensity plots of volatile products from TG of a polyimide prepreg as a function of temperature. (Reproduced with permission from ref. 99.)

ture. These results essentially confirm the previous conclusion of Figs. 32 and 33 (by the condensation method) that water and ethanol are involved in all weight loss steps. Chiu and Beattie [100] later described an improvement in this instrumentation's interface. Both the enrichment and yield were enhanced without much mass discrimination and the TG instrument could be operated under either a gas flow or vacuum and achieve quantitative analysis by both methods.

Lately, Dyszel [101] has described a combined TGA coupled with atmospheric pressure chemical ionization mass spectrometry. A diagram of the interface can be seen in Fig. 36 in which a TGS-2 TG analyzer is connected to a Sciex TAGA 3000 MS. An initial ionization occurs with the electron bombardment of nitrogen and the N_2^+ ion then undergoes a charge transfer reaction with oxygen, forming O_2^+. This species then forms a cluster with water vapor in the air and by a series of reactions forms the proton hydrate H_3O^+. As volatile products enter the ion source from the TG analyzer they react with the proton hydrates and either a proton or H_3O^+ is transferred to each molecule. The ionized molecules then pass through the quadrupole mass analyzer. This technique was applied to the analysis of a series of chemically modified and natural guar gums. These types of gums have been difficult to distinguish by TG methods alone due to their similar chemical compositions. However, by employing MS analysis the averaged mass spectral scans were sufficient to allow for distinction between the modified and unmodified food grade guar.

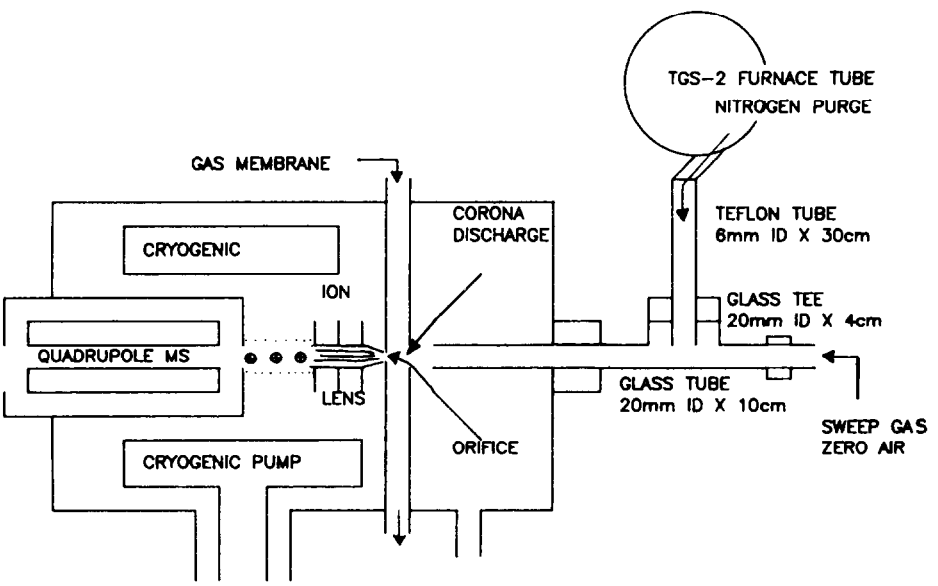

Fig. 36. Interface diagram of a TGS-2 TG analyzer coupled with a Sciex TAGA 3000 MS. (Reproduced with permission from ref. 101.)

(v) Combined techniques

This section will discuss the interfacing of multiple methods of thermal analysis to mass spectrometry. Only a few methods have been developed so far yet allow a wealth of information to be derived from a single sample run. Chang and Mead [102] coupled a TG analyzer to a gas chromatograph high resolution mass spectrometer with cold traps, in this tandem combination for trapping the evolved species. This combination provides thermal degradation of nonvolatile components by TGA, separation by GC and then identification by MS. The cold traps allow collection of the evolved gas components in one trap while analyzing the collected materials in the second trap. Figure 37 demonstrates the TGA of 3 mg of polystyrene foam and the loss of volatiles from the heated sample. The components were collected in one of the cold traps, volatilized and separated at once by GC, of which the chromatogram is presented in Fig. 38. Of the sixteen components separated by GC, Fig. 39 represents the recorded mass spectrum of one of these components (peak number 15). The GC peak was positively identified as that of the styrene dimer (M^+ 208). This instrumentation was also applied for similar analysis of an ethylene–vinyl acetate polymer as well. A system mentioned earlier was that of the combined method of Gibson and Johnson [72]. This combined instrument allowed for simultaneous measurement of TGA and DTA and was applied for analysis of geological samples. Müller-

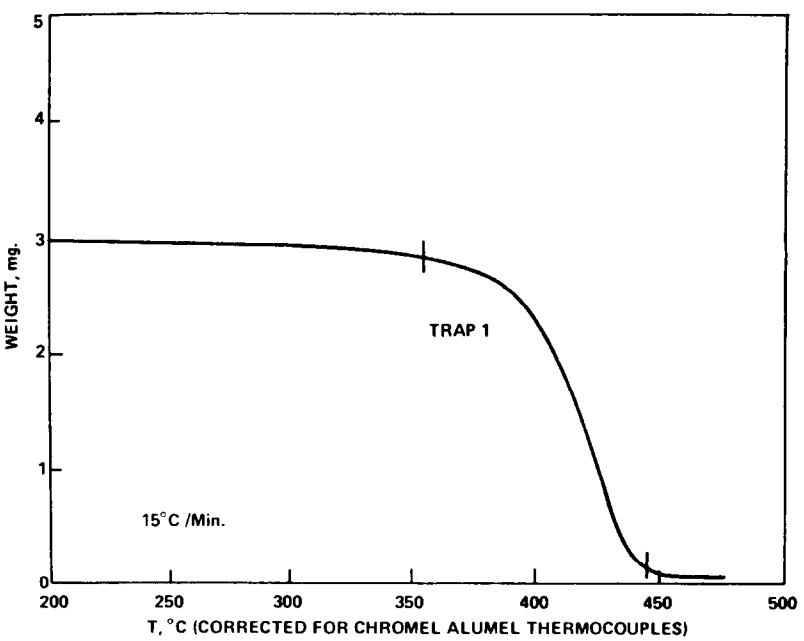

Fig. 37. TGA thermogram of polystyrene foam. (Reproduced with permission from ref. 102.)

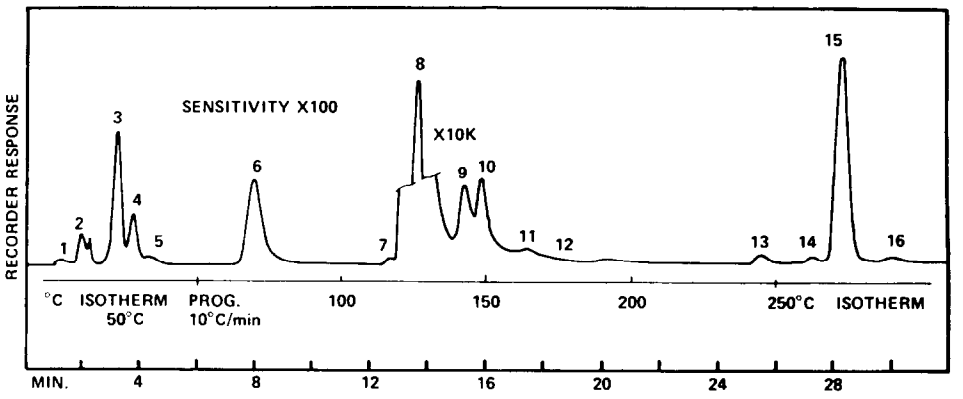

Fig. 38. GC chromatogram of effluent component from pyrolysis of polystyrene foam. (Reproduced with permission from ref. 102.)

Vonmoos et al. [103] developed a system which allowed for combined use of DTA, TG and evolved gas analysis with a quadrupole MS. This instrument was applied to the investigation of clay samples of complex mineralogical composition.

Others have described combined TGA-DTA-MS systems [104,105]. Kaisersberger [104] discussed some of the instrumental methods and their advantages and disadvantages among the various combined techniques and Dollimore et al. [105] applied this combined technique to the calculation of Arrhenius parameters for decomposition of nickel nitrate hexahydrate. The

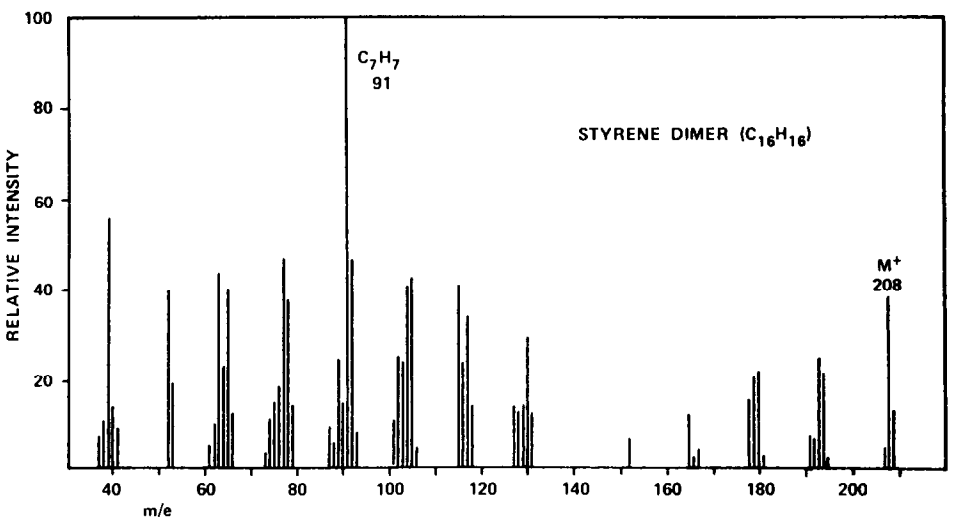

Fig. 39. Low resolution mass spectrum of peak number 15 from decomposition of polystyrene foam. (Reproduced with permission from ref. 102.)

latest technique described is that of Yuen et al [2] who developed an automated system which monitors simultaneous DTA, TG, DTG and MS under inert and oxidative atmospheres. Figure 40 presents a schematic diagram of the combined Mettler Thermoanalyzer and a Hewlett-Packard 5992 quadrupole mass spectrometer. The GC column inside the oven was replaced with a leak valve which could deliver 1×10^{-9} Torr s^{-1} and be heated to 450°C; gold-plated valves were used to avoid oxidation and contamination. The transfer line was heated by heating tape and monitored with a chromel–alumel thermocouple. A special quartz furnace was built for the thermoanalyzer and the interface between the furnace and mass spectral transfer line was accomplished with a 3/8 to 1/4 inch stainless steel swagelock union. Figure 41 represents a sample combined spectra that can be derived from this instrumentation for analysis of calcium oxalate monohydrate studied under a helium atmosphere. The masses observed as volatiles were water (*m/e* 18), carbon monoxide (*m/e* 28) and carbon dioxide (*m/e* 44) as the sample was heated to elevated temperatures. These results are plotted together with TG, DTG, and DTA chromatograms. There is excellent agreement in line shape between the DTG and mass ion peaks which suggests an insignificant dead-volume effect as the gases evolve; in each case, the DTG minimum and the mass ion maximum are seen to occur at the same temperature. Other samples were also applied for analysis by this system, such as styrene–butadiene diblock copolymer and other polymers.

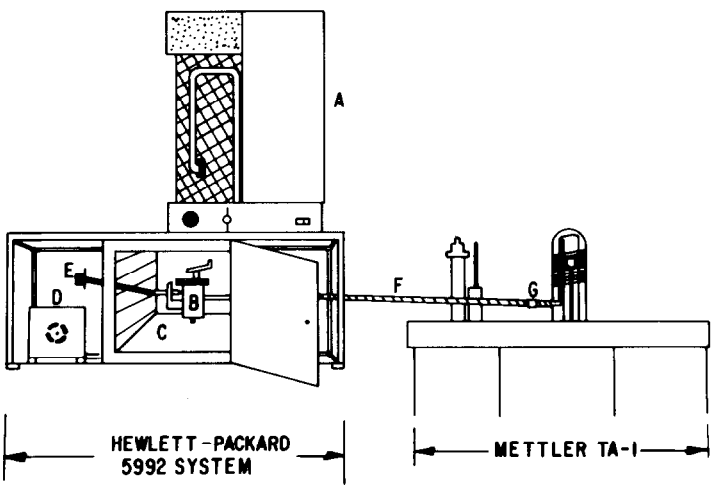

Fig. 40. A schematic diagram of the combined Mettler Thermoanalyzer and Hewlett-Packard 5992 quadrupole mass spectrometer. A, HP-5992 quadrupole mass spectrometer; B, Varian leak valve; C, GC oven; D, fore pump; E, leak valve fine adjustment control shaft; F, TA/MS transfer line; G, 3/8 in. to 1/4 in. s.s. Swagelock union. (Reproduced with permission from ref. 2.)

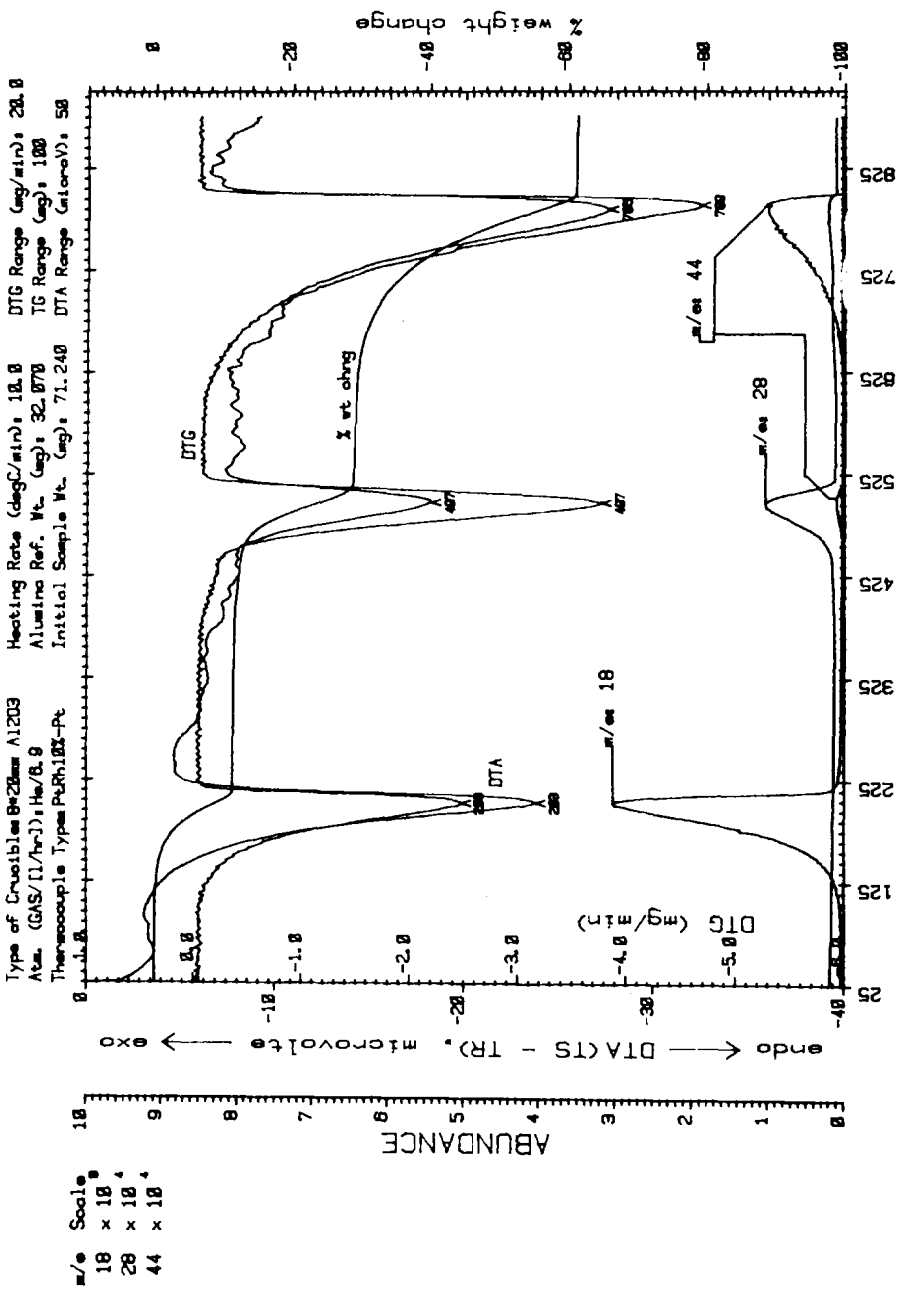

Fig. 41. DTA, TG and DTG thermograms plotted together with MS profiles for calcium oxalate monohydrate studied under a helium atmosphere. (Reproduced with permission from ref. 2.)

C. CONCLUSION

In this communication numerous methods of evolved gas analysis by mass spectrometry have been reviewed, along with selected applications. These techniques represent a number of advances that have been made in this field since the early reviews of Langer and Gohlke [3] in 1967 and Friedman [4] in 1970. Combinations of thermal analytical instrumentation with MS provides a powerful and unique means of analyzing and characterizing chemical and biological substances, whose properties may otherwise go unnoticed when observed by only one of the instrumental methods. Not only does this equipment provide qualitative data but a number of examples of quantitative applications have also been given.

REFERENCES

1 P.D. Zemany, Anal. Chem., 24 (1952) 1709.
2 H.K. Yuen, G.W. Mappes and W.A. Grote, Thermochim. Acta, 52 (1982) 143.
3 H.G. Langer and R.S. Gohlke, in W. Lodding (Ed.), Gas Effluent Analysis, Marcel Dekker, New York, Chap. 3, 1967.
4 H.L. Friedman, Thermochim. Acta, 1 (1970) 199.
5 H. Giacobbo and W. Simon, Pharm. Acta Helv., 39 (1964) 162.
6 H.L.C. Meuzelaar, J. Haverkamp and F.D. Hileman, Pyrolysis Mass Spectrometry of Recent and Fossil Biomaterials: Compendium and Atlas, Elsevier, Amsterdam, 1982, p. 6.
7 G.A. Charnock and J.L. Loo, Anal. Biochem., 37 (1970) 81.
8 D. Price, D. Dollimore, N.S. Fatemi and R. Whitehead, Thermochim. Acta, 42 (1980) 323.
9 H.L. Friedman, H.W. Goldstein and G.A. Griffith, Kinetics and Mechanisms of Thermal Degradation of Polymers Using Time of Flight Mass Spectrometry for Continuous Gas Analysis, Air Force Materials Laboratory, AFML-TR-68-11, 1969.
10 G.P. Shulman, Polym. Lett., 3 (1965) 911.
11 D. Dollimore, G.A. Gamlen and T.J. Taylor, Thermochim. Acta, 51 (1981) 269.
12 L. Carlsen and H. Egsgaard, Thermochim. Acta, 38 (1980) 47.
13 F.S. Karn, R.A. Friedel and A.G. Sharkey, Fuel, 51 (1972) 113.
14 R. Kaufman, F. Hillenkamp and E. Remy, Microsc. Acta, 73 (1972) 1.
15 R. Wechsung, F. Hillenkamp, R. Kaufman, R. Nitsche and H. Vogt, Mikroskopie, 34 (1978) 47.
16 W.J. Irwin, J. Anal. Appl. Pyrol., 1 (1979) 89.
17 W.J. Irwin, J. Anal. Appl. Pyrol., 3 (1981) 3.
18 V.G. Berezkin, Crit. Rev. Anal. Chem., 11 (1981) 1.
19 W.J. Irwin and J.A. Slack, Analyst (Amsterdam), 103 (1978) 1228.
20 J.F. Smith, Int. J. Mass Spectrom. Ion Phys., 26 (1978) 149.
21 D. Price, D. Dollimore, N.S. Fatemi and R. Whitehead, Thermochim. Acta, 42 (1980) 323.
22 S.A. Liebman and E.J. Lerry, J. Chromatogr. Sci., 21 (1983) 1.
23 T.P. Wampler, S.A. Liebman, E. Levy and S. Lamment, CDS Application Note, 6 (1981) 21.
24 G. Beech and R.M. Lintonbon, Thermochim. Acta, 3 (1971) 97.

25 T.B. Tang, Thermochim. Acta, 61 (1983) 341.
26 M.R. Udupa, Thermochim. Acta, 59 (1982) 21.
27 N.A. Bell, B.G. Hutley, J. Shelton and J.B. Turner, Thermochim. Acta, 21 (1977) 255.
28 W.E. Franklin, Anal. Chem., 51 (1979) 992.
29 K.C. Patil, J.P. Vittal and C.C. Patel, Thermochim. Acta, 43 (1981) 213.
30 G.K. Bratspies, J.F. Smith, J.O. Hill and R.J. Magee, Thermochim. Acta, 19 (1977) 349.
31 G.K. Bratspies, J.F. Smith, J.O. Hill and R.J. Magee, Thermochim. Acta, 19 (1977) 361.
32 G.K. Bratspies, J.F. Smith, J.O. Hill and R.J. Magee, Thermochim. Acta, 19 (1977) 335.
33 S. Morisaki, Thermochim. Acta, 9 (1974) 157.
34 E.P. Chang and R. Salovey, J. Polym. Sci., 12 (1974) 2927.
35 C.T. Vyayakumar and J.K. Fink, Thermochim. Acta, 59 (1982) 51.
36 E. Reiner, L.E. Abbey, T.F. Moran and R.W. Schafer, Biomed. Mass Spectrom., 6 (1979) 491.
37 R.L. Levy, Thesis, Israel Inst. Technol., Harfa, 1963.
38 W. Simon and H. Giacobbo, Chem. Ing. Technol., 37 (1965) 709.
39 H.L.C. Meuzelaar and P.G. Kistemaker, Anal. Chem., 45 (1973) 587.
40 H.L.C. Meuzelaar, 26th Ann. Conf. Mass Spectrom. Allied Topics, St. Louis, MO, May 28–June 2, 1978, p. 29.
41 H.L.C. Meuzelaar, P.G. Kistemaker, W. Eshuis and A.J.H. Boerboom, in N.R. Dailey (Ed.), Advances in Mass Spectrometry, Heyden, London, 1978, 7B, p. 1452.
42 W. Eshurs, P.G. Kistemaker and H.L.C. Meuzelaar, in C.E.R. Jones and C.A. Cramers (Eds.), Analytical Pyrolysis, Elsevier, Amsterdam, 1977, p. 151.
43 H.R. Schulten, H.D. Beckey, H.L.C. Meuzelaar and A.J.H. Boerboom, Anal. Chem., 45 (1973) 191.
44 L. Carlsen and H. Egsgaard, Thermochim. Acta., 38 (1980) 47.
45 A.J. Jason and A.C. Parr, Int. J. Mass Spectrom. Ion Phys., 22 (1976) 221.
46 H.D. Beckey, Field Ionization Mass Spectrometry, Pergamon Press, New York, 1971.
47 K. Levsen and H.D. Beckey, Org. Mass Spectrom., 9 (1974) 570.
48 L.W. Sieck, Anal. Chem., 51 (1979) 128.
49 H.J. Heinen, U. Gressman and F.W. Rollgen, Org. Mass Spectrom., 12 (1977) 710.
50 H.G. Langer and R.S. Gohlke, Anal. Chem., 35 (1963) 1301.
51 D.F. Anthrop and A.W. Searcy, J. Phys. Chem., 68 (1964) 2335.
52 G.P. Shulman, Polym. Lett., 3 (1965) 911.
53 C. Hirayama, R.L. Kleinosky and R.S. Bhalla, Thermochim. Acta, 39 (1980) 187.
54 P.K. Gallagher, Thermochim. Acta, 26 (1978) 175.
55 P.K. Gallagher, W.R. Sinclair, R.A. Fastnacht and J.P. Luongo, Thermochim. Acta, 8 (1978) 141.
56 P.K. Gallagher, Thermochim. Acta, 42 (1980) 323.
57 P.K. Gallagher and B. Prescott, Inorg. Chem., 9 (1970) 2510.
58 J.G. Brown, J. Dillimore, C.M. Freedman and B.H. Harrison, Thermochim. Acta, 1 (1970) 499.
59 R. Sakamoto, T. Ozawa and M. Kanazashi, Thermochim. Acta, 3 (1972) 291.
60 B. Pödor and I. Bertoti, Thermochim. Acta, 56 (1982) 209.
61 R.J. Comzemius and H.J. Svec, Anal. Chem., 50 (1978) 1854.
62 M.A. Posthumus, P.G. Kistemaker, H.L.C. Meuzelaar and M.C. Ten Noeverde Brauw, Anal. Chem., 50 (1978) 985.
63 D.M. Hercules, R.J. Day, K. Balasanmugam and C.P. Li, Anal. Chem., 54 (1982) 280A.
64 R.J. Comzemius and J.M. Capellen, Int. J. Mass Spectrom. Ion Phys., 34 (1980) 197.
65 F.J. Vastola, A.J. Pirone and B.E. Knox, Proc. 14th Ann. ASMS Conf. Mass Spectrom. Allied Topics, Dallas, TX, 1966, p. 78.
66 W.K. Joy, W.R. Ladner and E. Pritchard, Nature (Paris), 217 (1968) 640.
67 F.S. Karn, R.A. Friedel and A.G. Sharkey, Fuel, 51 (1972) 113.

68 G. Rhodes, R.B. Opsol, J.T. Meek and J.P. Reilly, Anal. Chem., 55 (1983) 280.
69 H.R. Schulten, P.B. Monkhouse and R. Miller, Anal. Chem., 54 (1982) 654.
70 P.G. Kistemaker, A.J.H. Boerboom and H.L.C. Meuzelaar, in D. Price and J.F.J. Todd (Eds.), Dynamic Mass Spectrometry, Vol. 4, Heyden, London, 1975, p. 139.
71 P.G. Kistemaker, H.H. Tuithof, A.J.H. Boerboom, B. Neering and H.L.C. Meuzelaar, in C.E.R. Jones and C.A. Cramers (Eds.), Analytical Pyrolysis, Elsevier, Amsterdam, 1977, p. 420.
72 R. Kaufmann, F. Hillenkamp and E. Remy, Microsc. Acta, 73 (1972) 1.
73 R. Nitsche, R. Kaufmann, F. Hillenkamp, E. Unsold, H. Vogt and R. Wechsung, Isr. J. Chem., 17 (1978) 181.
74 R.M. Lum, Thermochim. Acta, 18 (1977) 73.
75 C.H. Schiller, K.D. Kupka and F. Hillenkamp, Recent Developments in Mass Spectrometry in Biochemistry, Medicine and Environmental Research, Vol. 7, Elsevier, Amsterdam, 1980, p. 287.
76 N.E. Vanderborgh and C.E.R. Jones, Anal. Chem., 55 (1983) 527.
77 J.K. DeWasle, E.F. Vansant, P. Van Espen and F.C. Adams, Anal. Chem., 55 (1983) 671.
78 S.W. Graham, P. Dowd and D.M. Hercules, Anal. Chem., 54 (1983) 649.
79 K. Balasanmugam and D.M. Hercules, Anal. Chem., 55 (1983) 145.
80 B. Sprey and H.P. Bochem, Z. Anal. Chem., 308 (1981) 253.
81 U. Seydel and B. Lindner, Z. Anal. Chem., 308 (1981) 253.
82 H.G. Langer, R.S. Gohlke and D.H. Smith, Anal. Chem., 37 (1965) 433.
83 H.G. Langer and F.J. Karle, 15th Ann. Conf. on Mass Spectrom. Allied Topics, Denver, Colorado, May, 1967.
84 H.G. Langer and T.P. Brady, in R.F. Schwenker, Jr. and P.D. Garn (Eds.), Thermal Analysis, Vol. 1, Academic Press, New York, 1969, p. 295.
85 J.P. Redfern, B.L. Treherne, M.L. Aspimol and W.A. Wolsenholme, 17th Ann. Conf. on Mass Spectrom. Allied Topics, Dallas, TX, May, 1969.
86 C.A. Gaulin, F. Wachi and T.H. Johnson, in R.F. Schuenber, Jr. and P.D. Garn (Eds.), Thermal Analysis, Vol. 2, Academic Press, New York, 1969, p. 1453.
87 W.W. Wendlandt, T.M. Southern and J.R. Williams, Anal. Chim. Acta, 35 (1966) 254.
88 W.W. Wendlant, Thermal Methods of Analysis, Vol. 19, John Wiley, New York, 2nd edn., 1974, p. 348.
89 H.G. Langer and T.P. Brady, Thermochim. Acta, 5 (1973) 391.
90 D. Dollimore, J.P. Gupta, N.J. Manning and D.V. Nowell, Thermochim. Acta, 31 (1979) 357.
91 F. Zitomer, Anal. Chem., 40 (1968) 1091.
92 E.K. Gibson, Jr. and S.M. Johnson, Thermochim. Acta, 4 (1972) 49.
93 H.G. Weideman, Chem. Ing. Tech., 36 (1964) 1105.
94 E.K. Gibson, Jr., Thermochim. Acta, 5 (1973) 243.
95 G.J. Mol, Thermochim. Acta, 10 (1974) 259.
96 J. Chiu and A.J. Beattie, Thermochim. Acta, 21 (1977) 263.
97 E. Baumgartner and E. Nachbaur, Thermochim. Acta, 19 (1977) 3.
98 H. Eppler and H. Selhofer, Thermochim. Acta, 20 (1977) 45.
99 J. Chiu and A.J. Beattie, Thermochim. Acta, 40 (1980) 251.
100 J. Chiu and A.J. Beattie, Thermochim. Acta, 50 (1981) 49.
101 S.M. Dyszel, Thermochim. Acta, 61 (1983) 169.
102 T.L. Chang and T.E. Mead, Anal. Chem., 43 (1971) 534.
103 M. Müller-Vonmoos, G. Kahr and A. Rub, Thermochim. Acta, 20 (1977) 387.
104 E. Kaisersberger, Thermochim. Acta, 29 (1979) 215.
105 D. Dollimore, G.A. Gamlen and T.J. Taylor, Thermochim. Acta, 51 (1981) 269.